

University of Leicester
Department of Physics and Astronomy
Lecture Notes
Lasers and Quantum Optics

Prof. R. Willingale

December 6, 2011

Contents

1	Books	4
2	Introduction	4
2.1	Coherence - quantum cooperation	5
2.2	Polarization - angular momentum	11
2.3	Fields and photons	14
2.4	Classical field theory	14
2.5	Quantum field theory	14
2.6	Properties of photons	15
3	Lasers	16
3.1	Stimulated emission - cloning photons	16

3.2	Population inversion	18
3.3	Pumping - 3 and 4 level systems	18
3.4	Optical feedback - resonant cavities	20
3.5	Line broadening	23
3.6	Laser modes	24
3.7	The hallmarks of laser activity	25
4	Types and classes of laser	28
4.1	Doped insulator lasers	28
4.2	Semiconductor lasers	30
4.3	Atomic gas lasers	32
4.4	Ion lasers	34
4.5	Molecular lasers- the carbon dioxide laser	36
4.6	Liquid dye lasers	36
4.7	The free electron laser	39
4.8	The properties of laser light	43
5	Photon statistics	44
6	Optical wave guides - fibre optics	45
6.1	Planar wave guides - a simple wave model	47
6.2	The uncertainty principle	49
6.3	Polarization states	49
6.4	Rays in a cylindrical cladded fibre	52

6.5	Fibre optics	54
6.6	Step index and graded index fibres	57
6.7	Dispersion in fibre optics	57
6.8	Losses in fibre optics	59
6.9	Communication using fibre optics	61
6.10	Communication examples	62
7	Polarization	62
7.1	The linear polarizer	62
7.2	The law of Malus	62
7.3	Dichroic crystals	63
7.4	Complex refractive index	64
7.5	The wire grid polarizer	64
7.6	Dichroic sheet - Polaroid	65
7.7	Polarization by scattering - dipole scattering	65
7.8	Polarization by reflection	67
8	Optical anisotropy	69
8.1	Birefringence - double refraction	69
8.2	Optical activity	72
8.3	Retarders	74
9	Induced optical anisotropy	75
9.1	Faraday rotation - magnetically induced optical activity	75

9.2	Liquid crystals	78
9.3	The Kerr and Pockels effects	81
10	Nonlinear optics	83
10.1	Solitons	83
10.2	Frequency doubling and mixing	85

1 Books

- Optics and Photonics An Introduction, F.G.Smith and T.A.King, Wiley
- Optoelectronics: An introduction, Second edition. J.Wilson and J.F.B.Hawkes, Prentice Hall
- Insight into Optics, O.S.Heavens and R.W.Ditchburn, Wiley
- Principles of Optical Engineering, F.T.S.Yu and I.C.Khoo, Wiley
- Optical Coherence and Quantum Optics, Leonard Mandel and Emil Wolf, CUP
- Principles of Optics, 7th edition, Max Born and Emil Wolf, CUP

2 Introduction

There are 4 underlying forces at work in physics

- gravity
- electromagnetic
- strong nuclear
- weak nuclear

Gravity is only important in large scale phenomena.

The strong and weak nuclear forces only come into play in nuclear physics when we deal with the very microscopic world and high quantum energies. e.g. radioactivity

The electrostatic force between 2 protons is $10^{38} >$ gravitational attraction. The electromagnetic interaction between electrons (charge) and photons dominates in almost all commonly observed phenomena. Therefore classical electromagnetism or quantum electrodynamics are at the heart of much of physics.

Light is electromagnetic and the physics of light, optics, is central to many physical situations. We are interested in how light behaves and ultimately we want to answer the question "What is light?" In order to study light we must concern ourselves with a large number of subjects, for example:

- electromagnetism
- quantum mechanics
- thermodynamics
- atomic physics
- solid state physics
- relativity

There are 2 threads in the course:

- principles of optics - the theoretical modelling of light - what is it?
- photonics - optical devices and applications - making light work

2.1 Coherence - quantum cooperation

Coherence is associated with the wave like nature of light. It manifests itself in interference and/or diffraction effects.

Temporal coherence and the harmonic content of the wave at a fixed point in space.

Perfect temporal coherence $f(t) = A \exp(i\omega_0 t)$

Take Fourier transform $F(\omega) = C\delta(\omega - \omega_0)$

Only 1 frequency is present and the wave is continuous in time. In practice the length of the wave is finite, a pulse of length Δt . This leads to a spread in frequency:

$$\Delta f \approx 1/\Delta t = \Delta\omega/2\pi$$

For a Gaussian wavepacket we have:

$$f(t) = A \exp(i\omega_0 t) \exp(-t^2/2\Delta t^2)$$

$$F(\omega) = B \exp(-\Delta t^2(\omega_0 - \omega)^2/2)$$

If have successive wave packets arriving randomly then:

$$C(t) = \sum_{m=1}^n A_m \exp(i\omega(t - t_m)) \exp(-(t - t_m)^2/2\Delta t^2)$$

and the resulting amplitude is $\propto n^{1/2}$.

If all the same length and frequency then still get the same bandwidth.

Can express a bandwidth or coherence time using a coherence length. This amounts to taking a snapshot of the packet as it passes and measuring its length. If the coherence time is Δt then length of packet in direction of travel must be $c\Delta t = \Delta x$.

The concept of coherence length is important in amplitude splitting interference devices such as the Michelson Interferometer.

We can also study the coherence of light perpendicular to the direction of travel. This is known as *lateral coherence* or *spatial coherence* and is important in wavefront splitting interference such as seen from Young's slits.

The combination of temporal and lateral coherence define a *coherence volume*.

We characterise or quantify coherence using *correlation functions*. Such correlations are found by taking *time averages* of the wave. This removes fluctuations due to the discrete wave trains or packets.

When we calculate interference or diffraction patterns we are finding correlation functions. We combine component complex amplitudes arising from both the temporal (frequency) and spatial (wavelength) characteristics of the travelling wave.

Likewise when we measure interference or diffraction patterns the form of the distribution tells us something about the coherence of the light. Different degrees of coherence are illustrated in Figs. 1, 2,3 and 4.

Perfect coherence

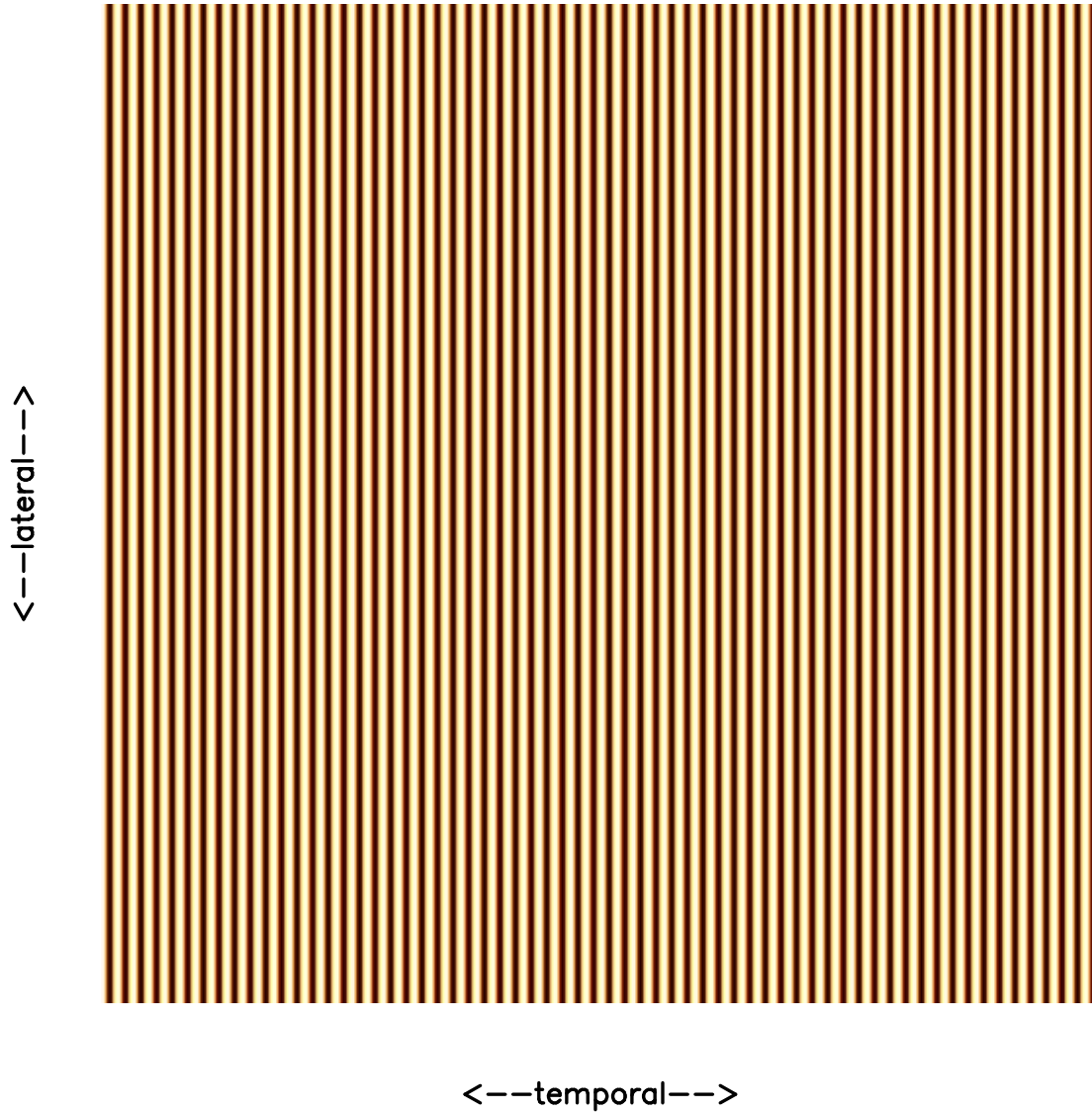


Figure 1: Perfect coherence

equal temporal and lateral coherence

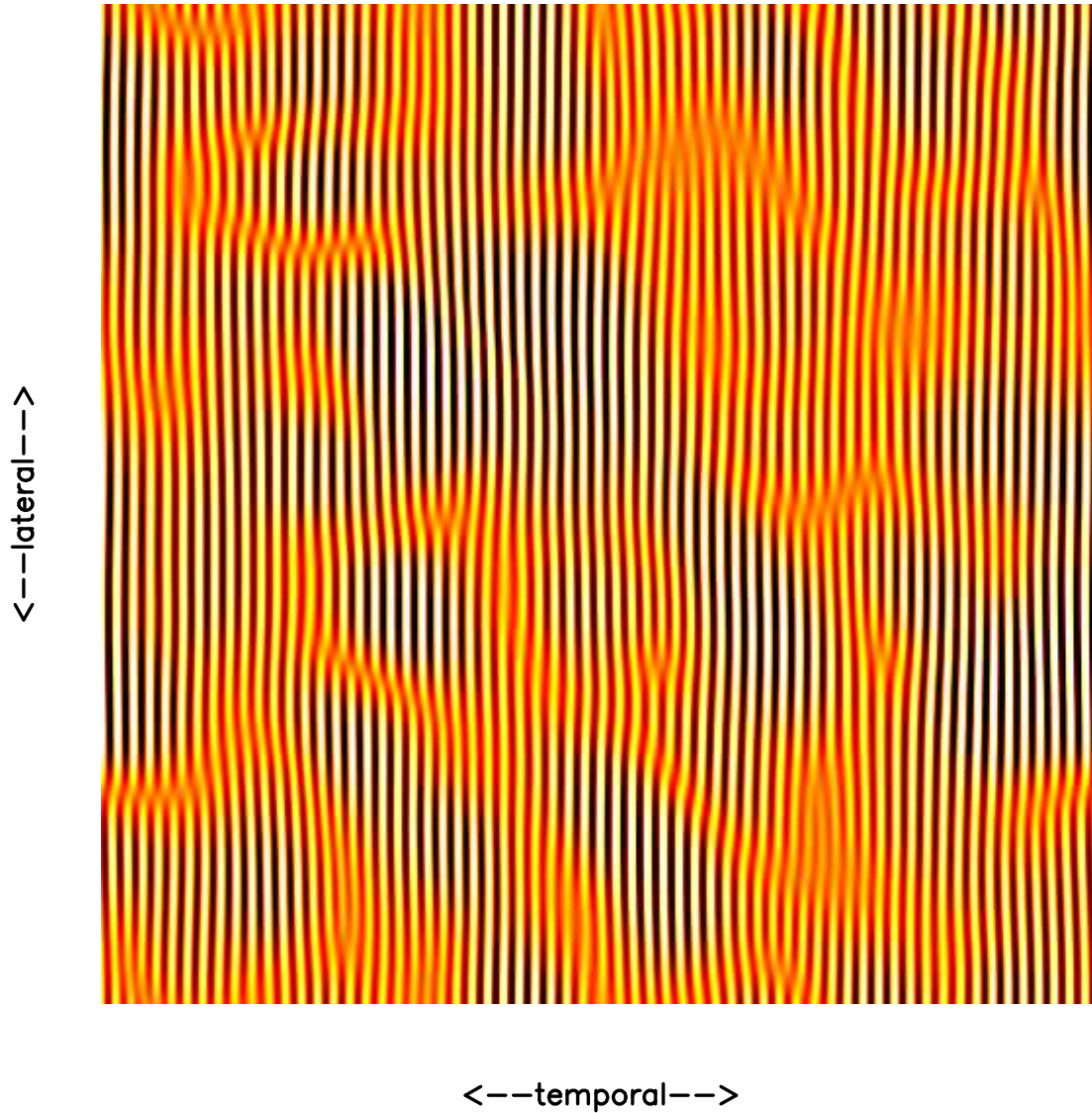


Figure 2: Equal temporal and lateral coherence

high lateral low temporal coherence

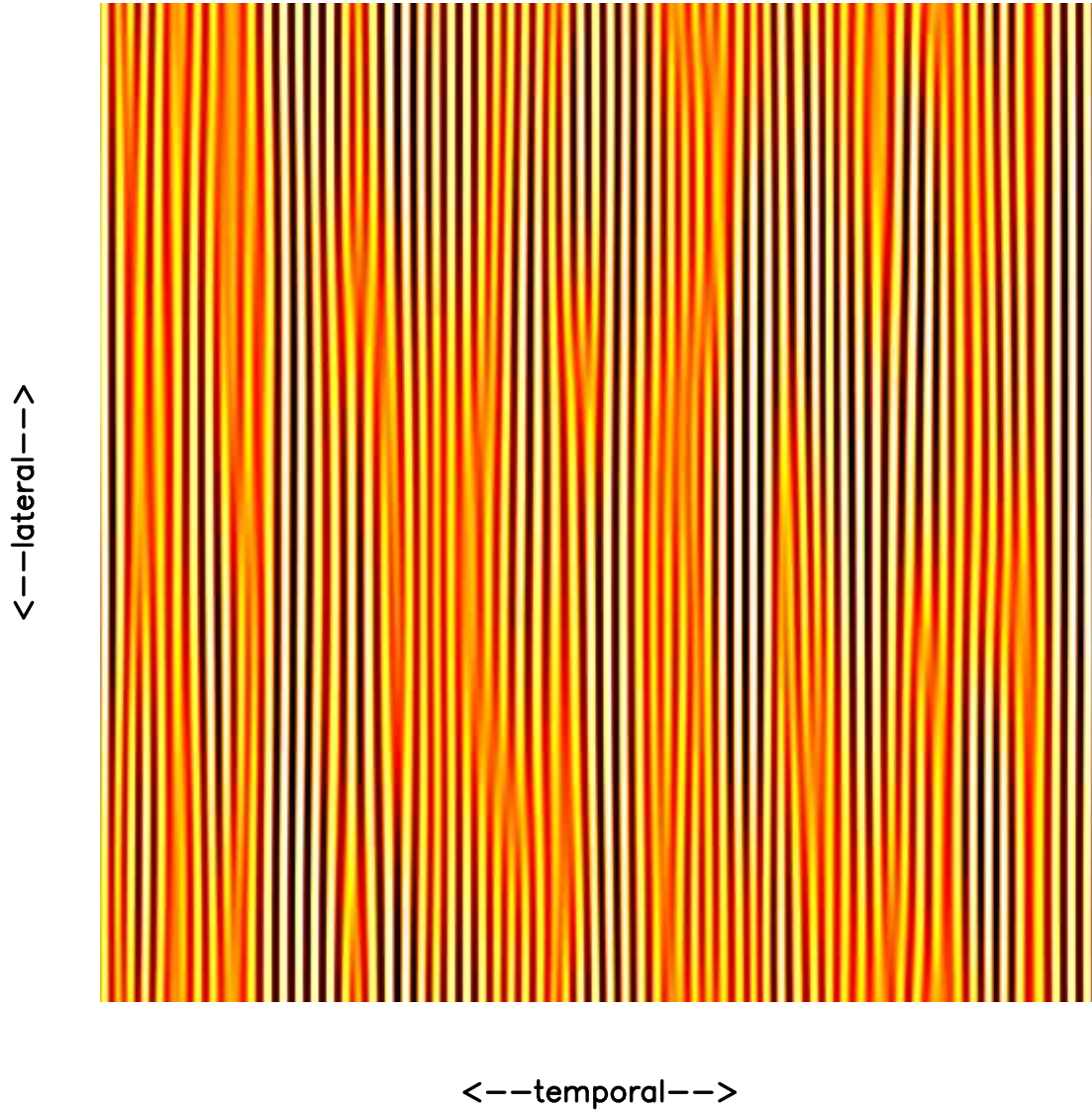


Figure 3: High lateral and low temporal coherence

high temporal low lateral coherence

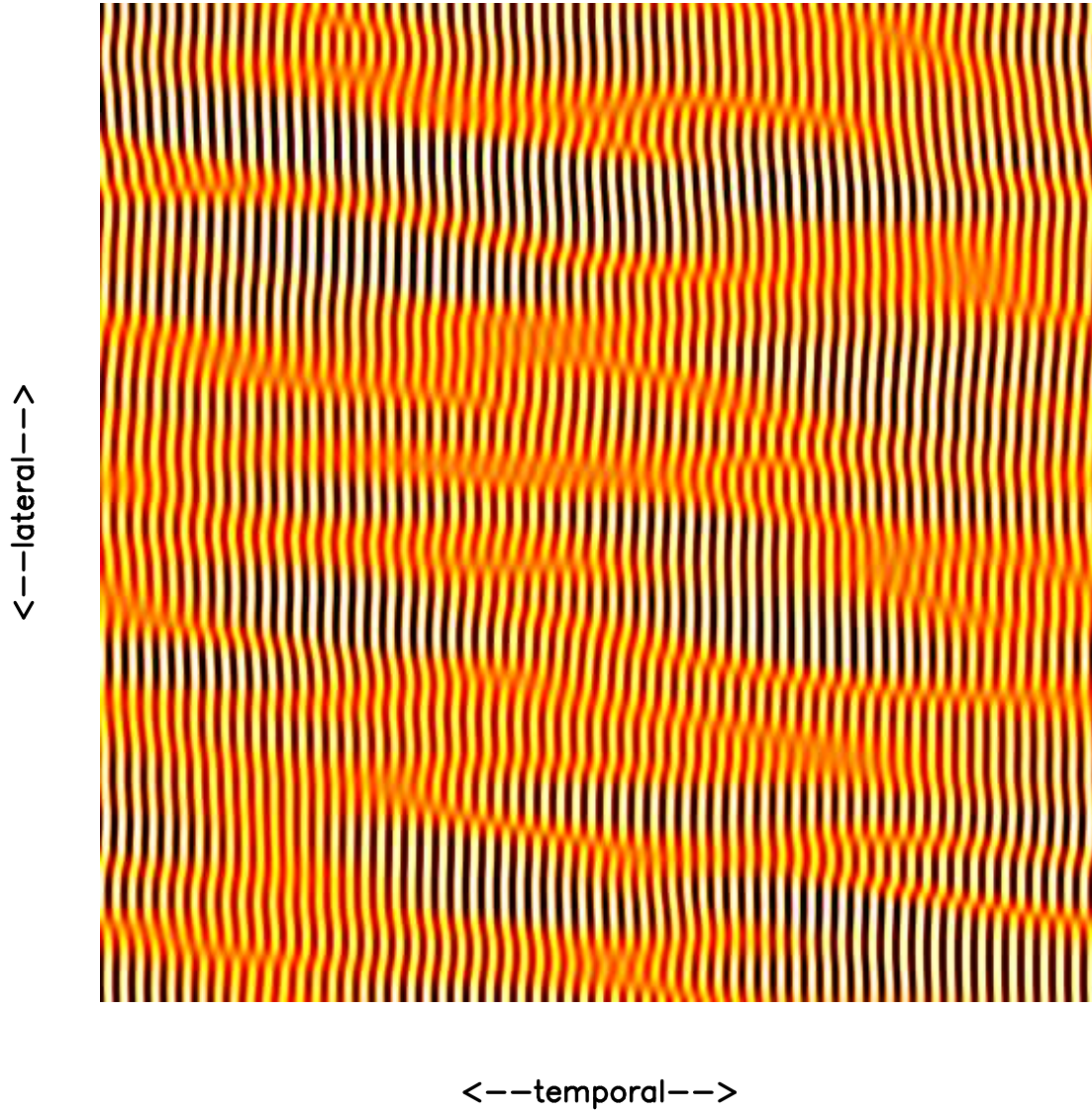


Figure 4: High temporal and low lateral coherence

2.2 Polarization - angular momentum

The polarization of light is described using different polarization states:

- P - linear light (plane polarized)
- R - right hand circular
- L - left hand circular

Natural light has a random polarization as a function of time.

Plane polarized light can be described as a linear combination of right and left states $P = L + R$. The electric field components of the P-state are shown in Fig. 5.

Circular light can be described as the summation of 2 orthogonal P states out of phase by $\pi/2$. The electric field components of the R-state are shown in Fig. 6.

The polarization of light is important in reflection, scattering, birefringence, optical activity.

Retarders and polarizers can be used to convert between states,

$P \leftrightarrow R \text{ or } L$

What happens to electrons exposed to circular light? Using the 2 P state picture we see that the electron is driven sinusoidally in 2 orthogonal directions but with a $\pi/2$ phase difference. Therefore a free electron will move in a circle with angular frequency ω . Thus *angular momentum* is imparted to the electron.

The power delivered is the rate of energy dissipation $d\mathcal{E}/dt$ and this is equal to the product of the torque \mathcal{T} and ω

$$d\mathcal{E}/dt = \mathcal{T}\omega$$

But $\mathcal{T} = d\mathcal{L}/dt$ is the rate of change of angular momentum. Therefore assuming all the light (photon) energy is absorbed by the electron we can integrate giving

$$\mathcal{L} = \mathcal{E}/\omega$$

R or L states have associated angular momenta described by vectors. The R state rotates clockwise looking towards the source and is represented by \vec{R} pointing away from the

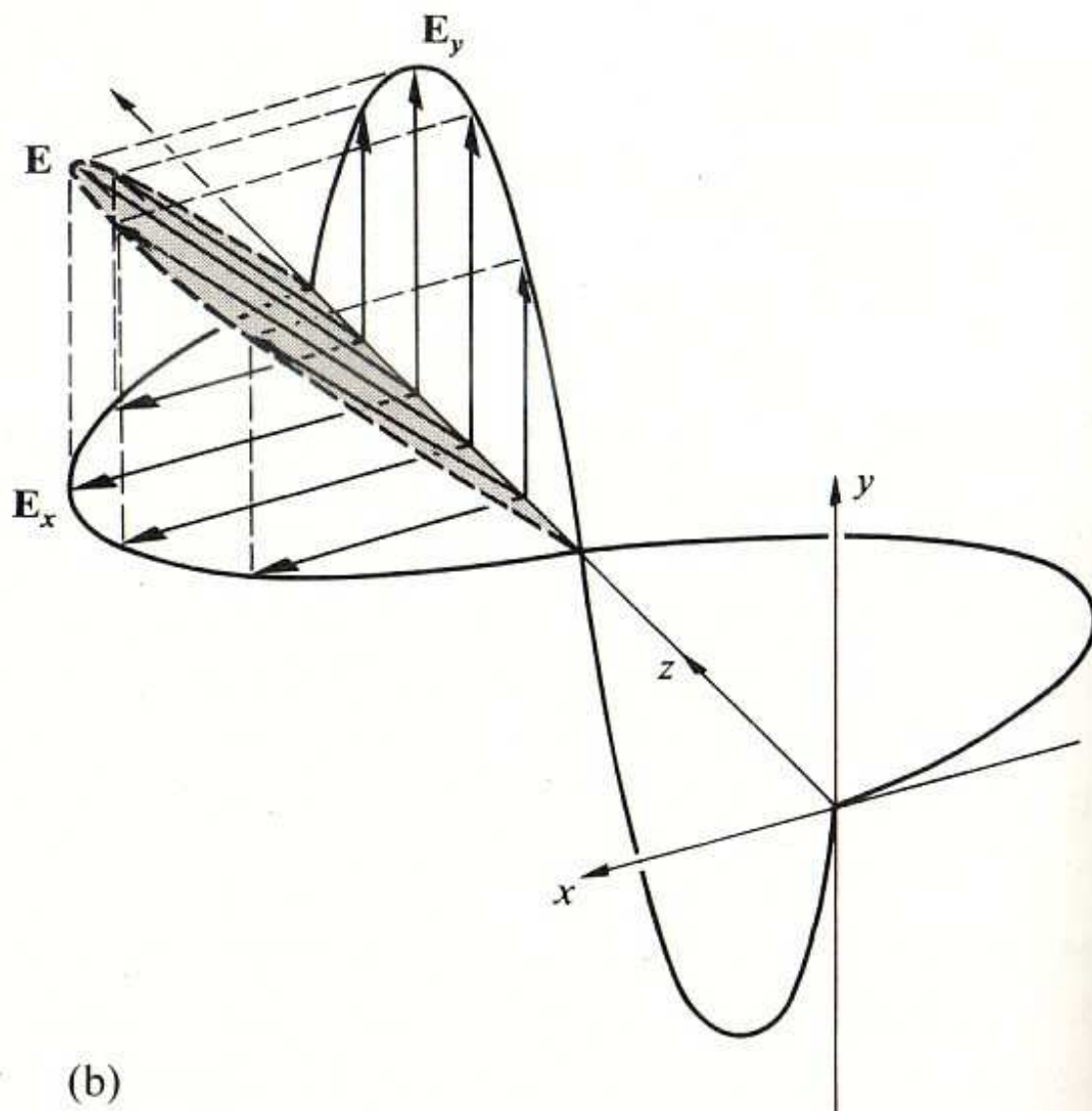


Figure 5: P-state of polarization

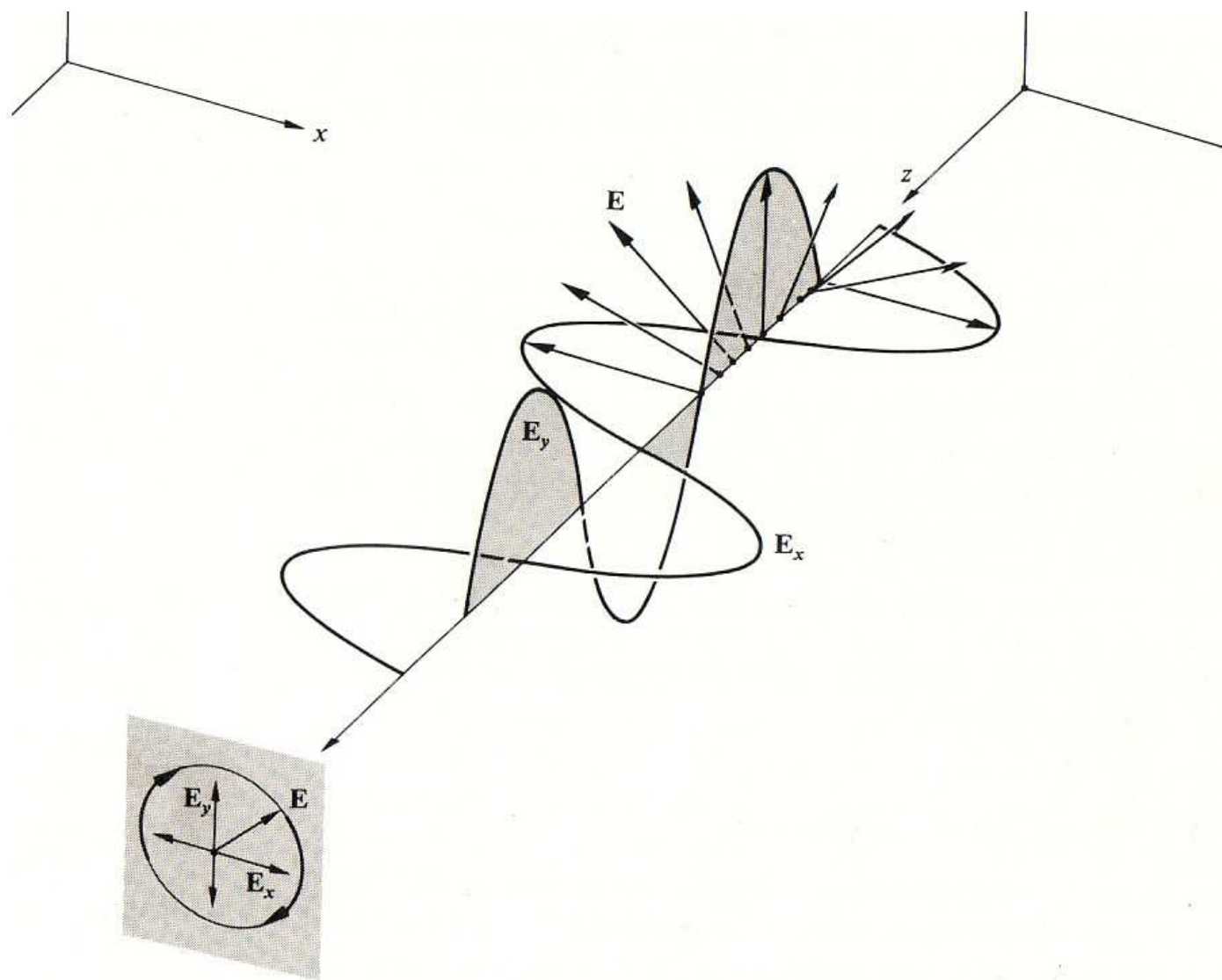


Fig. 8.3 Right circular light.

Figure 6: R-state of polarization

source. The L state is represented by \vec{L} a vector pointing towards the source (opposite to the \vec{k} wave vector).

2.3 Fields and photons

A *light beam* has coherence that depends on the nature and geometry of the source and region of propagation. The coherence depends on the bandwidth $\Delta\omega$ which in turn depends on the energy bandwidth ΔE .

A *light beam* has a polarization and carries angular momentum.

A *light beam* carries energy - irradiance - associated with the square of the amplitude of the electric field vector.

How are these properties tied up with the emission and absorption processes?

2.4 Classical field theory

Described by Maxwell's equations. Charge, stationary and moving, generates electric and magnetic fields which in turn impose forces on other charge (Lorentz force). The classical E-M field is physical, it is not just a mathematical trick to calculate the forces between charges.

Consider a parallel plate capacitor charged up with a vacuum between the plates. There is an E-field in the gap. Now imagine the plates are moved apart. This requires work to be done against the attractive force between the 2 sheets of charge on the plates. Afterwards the plates etc. look exactly the same. The only change is that there is a greater volume of vacuum between the plates. Yet work has been done and more energy is stored in the system. This energy is in the electric field between the plates. The field contains energy and has an equivalent mass given by $E = mc^2$. There is no *ether* to support the field and it has energy (or mass) as *real* as any other stuff.

2.5 Quantum field theory

All interactions involve the creation and annihilation of particles. Forces come about through the exchange of lumps of energy or *quanta of the field* in question. The field itself is quantized. Classically we describe interference by summing electric field amplitudes and finding the intensity by calculating $|amp|^2$.

In QFT we consider the probabilities of particles arriving at some point from a source. These probabilities (or probability densities) are calculated from wave functions $Prob = |\phi|^2$. We sum the probabilities in the following way $\phi = \phi_1 + \phi_2 + \phi_3 + \dots$. Then

$$Prob = |\phi_1 + \phi_2 + \phi_3 + \dots|^2$$

$$NOT\ Prob = |\phi_1|^2 + |\phi_2|^2 + |\phi_3|^2 + \dots$$

This process naturally leads to interference. Consider a beam reflecting off a plane mirror. We must sum the probabilities over all possible paths in a similar way to the application of Fermat's principle. In the summation it is only contributions near to the *classical* reflection point that add up in phase. The contributions from the various points over the mirror surface stack together like a *Cornu spiral*. Contributions from remote areas of the mirror surface or an aperture are small and have little effect on the resultant probability. We only start to see interference effects when the dimension of the mirror or aperture become comparable to the wavelength of the functions ϕ_n .

So our classical E-M field becomes a quantized field which describes the *probability of detecting a photon*.

2.6 Properties of photons

They carry energy $\mathcal{E} = h\nu$

They carry momentum $\mathcal{P} = (\mathcal{E}^2 - m_0^2 c^4)^{1/2} / c$

But $m_0 = 0$, zero rest mass, so $\mathcal{P} = \mathcal{E} / c = h / \lambda$

They carry angular momentum $|\mathcal{L}| = \mathcal{E} / \omega = \pm \hbar$

where \pm refer to the R and L polarization states or *photon spin*.

So emission of photons puts energy, momentum and angular momentum into the quantum field in lumps and absorption removes them from the field in lumps.

Is the *quantum field* real?

Of course. A photon detector placed in such a field (light beam), receives energy, momentum and angular momentum from the field. The detector feels the beam!

Coherence is quantum cooperation. A very large number of photons are in the same state. This is possible because photons are *bosons* with spin ± 1 . They are force carriers.

Interference. Photons can only interfere with themselves. Different photons NEVER interfere. So different sources of photons don't interfere. Interference between sources is done by splitting the field from a single source. You can set up Young's slits with such a low intensity of light that at any time only 1 photon is interacting with the slits. It still works.

Polarization. When a photon is detected it can be in a R or L state (spin ± 1). Therefore you can extract angular momentum from a circularly polarized beam.

3 Lasers

3.1 Stimulated emission - cloning photons

A photon is emitted when an electron in an atom undergoes a transition between 2 energy levels.

$$\nu = \Delta\mathcal{E}/h = (\mathcal{E}_2 - \mathcal{E}_1)/h$$

This can occur in 2 ways:

- Spontaneous emission - random - governed by a lifetime τ_{21}
- Stimulated emission - in the presence of a stimulating photon. The emitted photon has the same \mathcal{E} , \mathcal{P} and \mathcal{L} as the stimulating photon. It has the same ν and polarization state.

We normally only see spontaneous emission. This requires just an atom rather than an atom plus a photon and consequently the transition probability is usually much higher.

The opposite process, absorption, always requires a photon plus an atom and it is really the reverse of stimulated emission.

Stimulated emission was demonstrated to exist by Einstein in 1917. It can be regarded as a resonance phenomenon. We can derive relationships between the processes by considering a simple system in thermal equilibrium.

In equilibrium the average number of upward transitions must equal the average number of downward transitions. Let N_1 be the number density of atoms in the low state and N_2 be the number density in the high state. Let ρ_ν be the energy density of the light at frequency ν .

$\rho_\nu = N_\nu h\nu$ where N_ν is the number of density of photons per unit frequency interval.

There are 3 transition rates:

- $N_1\rho_\nu B_{12}$ upwards due to absorption
- $N_2\rho_\nu B_{21}$ downwards due to stimulated emission
- N_2A_{21} downwards due to spontaneous emission

In equilibrium $N_1\rho_\nu B_{12} = N_2\rho_\nu B_{21} + N_2A_{21}$

$$\text{or } \rho_\nu = \frac{A_{21}/B_{21}}{(B_{12}N_1/B_{21}N_2)-1}$$

In thermal equilibrium Boltzman statistics give:

$$N_j = \frac{g_j N_0 \exp(-\mathcal{E}_j/kT)}{\sum_i g_i N_i \exp(\mathcal{E}_i/kT)}$$

where N_0 is the total population density and N_j is the occupancy and g_j is the degeneracy of the j th level. Using this we get:

$$N_1/N_2 = (g_1/g_2) \exp(h\nu/kT)$$

But ρ_ν is also given by the Planck distribution for black-body radiation:

$$\rho_\nu = \frac{8\pi h\nu^3}{c^3} \frac{1}{\exp(h\nu/kT)-1}$$

So equating the 2 expressions for ρ_ν gives us

$$g_1 B_{12} = g_2 B_{21} \text{ and } A_{21}/B_{21} = 8\pi h\nu^3/c^3$$

These are known as the Einstein relations and A_{12} , B_{12} and B_{21} are called the Einstein coefficients. The ratio of spontaneous to stimulated emission is given by

$$R = A_{21}/\rho_\nu B_{21} = \exp(h\nu/kT) - 1$$

For example in a hot filament at 2000K with $\nu \approx 5 \times 10^{14}$ then $R = 1.5 \times 10^5$. Stimulated emission is completely swamped by spontaneous emission.

In order to boost the stimulated component we must increase N_2/N_1 and ρ_ν . This is achieved in the LASER process - *Light Amplification by Stimulated Emission of Radiation*.

3.2 Population inversion

Imagine we have a collimated, monochromatic beam passing through an absorbing medium containing just 1 relevant transition $\mathcal{E}_2 \leftrightarrow \mathcal{E}_1$ with $\nu_{12} = (\mathcal{E}_2 - \mathcal{E}_1)/h$.

If α is the absorption coefficient

$$dI(x)/dx = -\alpha I(x) \implies I = I_0 \exp(-\alpha x)$$

Ignoring scattering losses and spontaneous emission which is isotropic

$$-dN_\nu/dt = N_1\rho_\nu B_{12} - N_2\rho_\nu B_{21}$$

$$\text{so } -dN_\nu/dt = (g_2 N_1/g_1 - N_2)\rho_\nu B_{21}$$

If n is the refractive index $I_\nu = \rho_\nu c/n = N_\nu h\nu_{12}c/n$

$$\Delta N_\nu(x) = \Delta x \frac{dI_\nu}{dx} n / h\nu_{12}c$$

but $\Delta t = \Delta x n/c$ so we get

$$dN_\nu/dt = \frac{dI_\nu}{dx} \frac{1}{h\nu_{12}} = -\alpha I_\nu / h\nu_{12}$$

$$dN_\nu/dt = -\alpha \rho_\nu c / n h\nu_{12}$$

Therefore α is given by

$$\alpha = (g_2 N_1/g_1 - N_2) B_{21} h\nu_{12} n / c$$

If α is negative $N_2 > g_2 N_1/g_1$ and the beam intensity will increase exponentially $I = I_0 \exp(\kappa x)$ where

$\kappa = -\alpha$ is called the *small signal gain*.

To get positive gain we require a *population inversion*. Such an inversion requires energy from a *pumping* process. The pumping produces *nonthermal* equilibrium.

3.3 Pumping - 3 and 4 level systems

Because $B_{21} = B_{12}$ we must use a third level to get $N_2 > g_2 N_1/g_1$.

Pumping is into an energy level above the top level of the LASER transition. This level must decay rapidly to fill the top level. Often the pumped levels consist of a band which give a high level of absorption to a wide spectrum.

The 3 level system is inefficient because the lower level of the LASER transition is always populated.

A 4 level system is much more efficient. In this case the population in \mathcal{E}_1 will be low providing $\mathcal{E}_1 - \mathcal{E}_0 > kT$.

The 3 and 4 level systems are illustrated in Figs. 7 and 8. In each case the left-hand diagram shows the distribution at thermal equilibrium (Boltzman) and the right-hand diagram shows the distribution with pumping. In order to achieve and maintain a

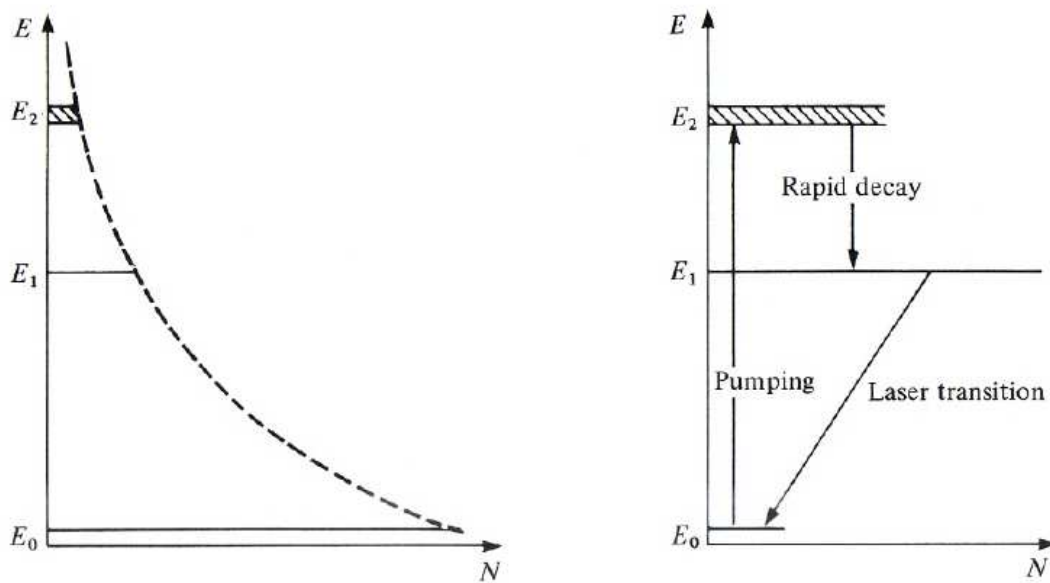


Figure 7: 3 level laser system

population inversion we must excite electrons into the short lifetime levels above the upper LASER level. There are a number of ways this can be done.

- Optical pumping - use an intense flash of white light. Use reflectors etc. to concentrate as much of this light into the LASER beam volume.
- Electric current. Power source used directly in semiconductor lasers.
- D.C. discharge. Used in gas lasers.
- Gas dynamic discharge - uses thermodynamic properties of gas - push gas through a compression-expansion cycle.

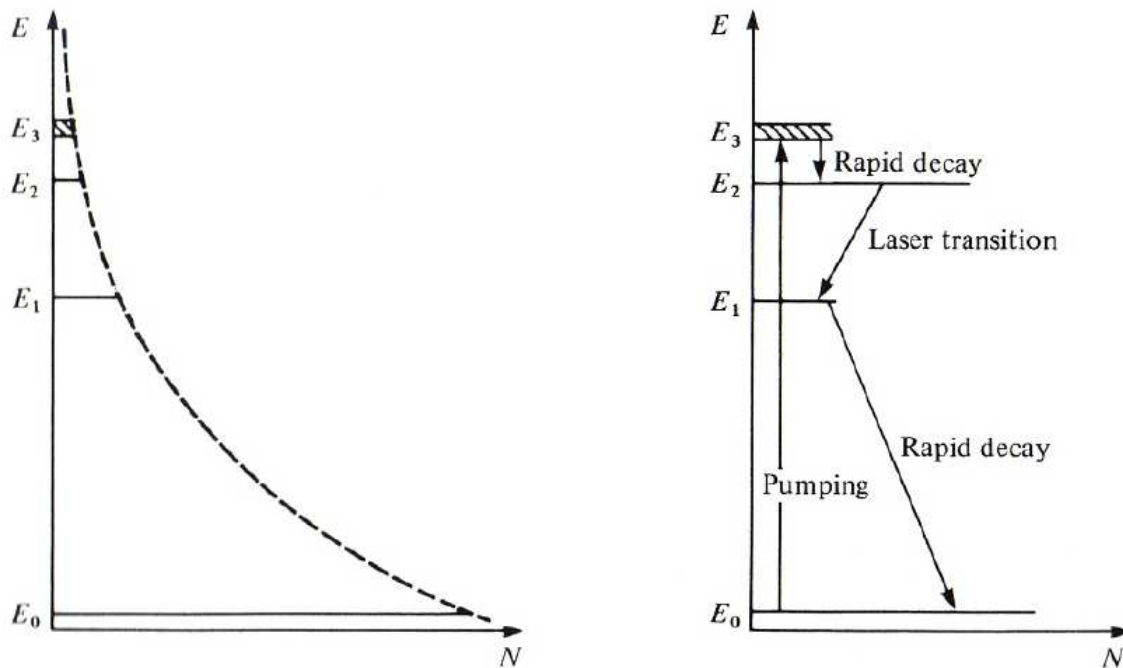


Figure 8: 4 level laser system

- Laser pumping by other lasers.

3.4 Optical feedback - resonant cavities

The LASER scheme described so far amplifies the light beam but the gain per unit length in the active medium is usually rather small. To get large gains we need a long path all of which is pumped. A neat way of getting this is to fold the beam on itself by reflection between 2 mirrors. This traps the beam in a resonant cavity often called a *Fabry Perot Resonator*.

Different forms of cavity are used for different applications:

- plane plane - this produces a large mode volume but is difficult to make because the mirrors must be flat and parallel.
- large r_1 large r_2 - gives maximum power
- confocal - very easy to align
- hemispherical - can get good coherence

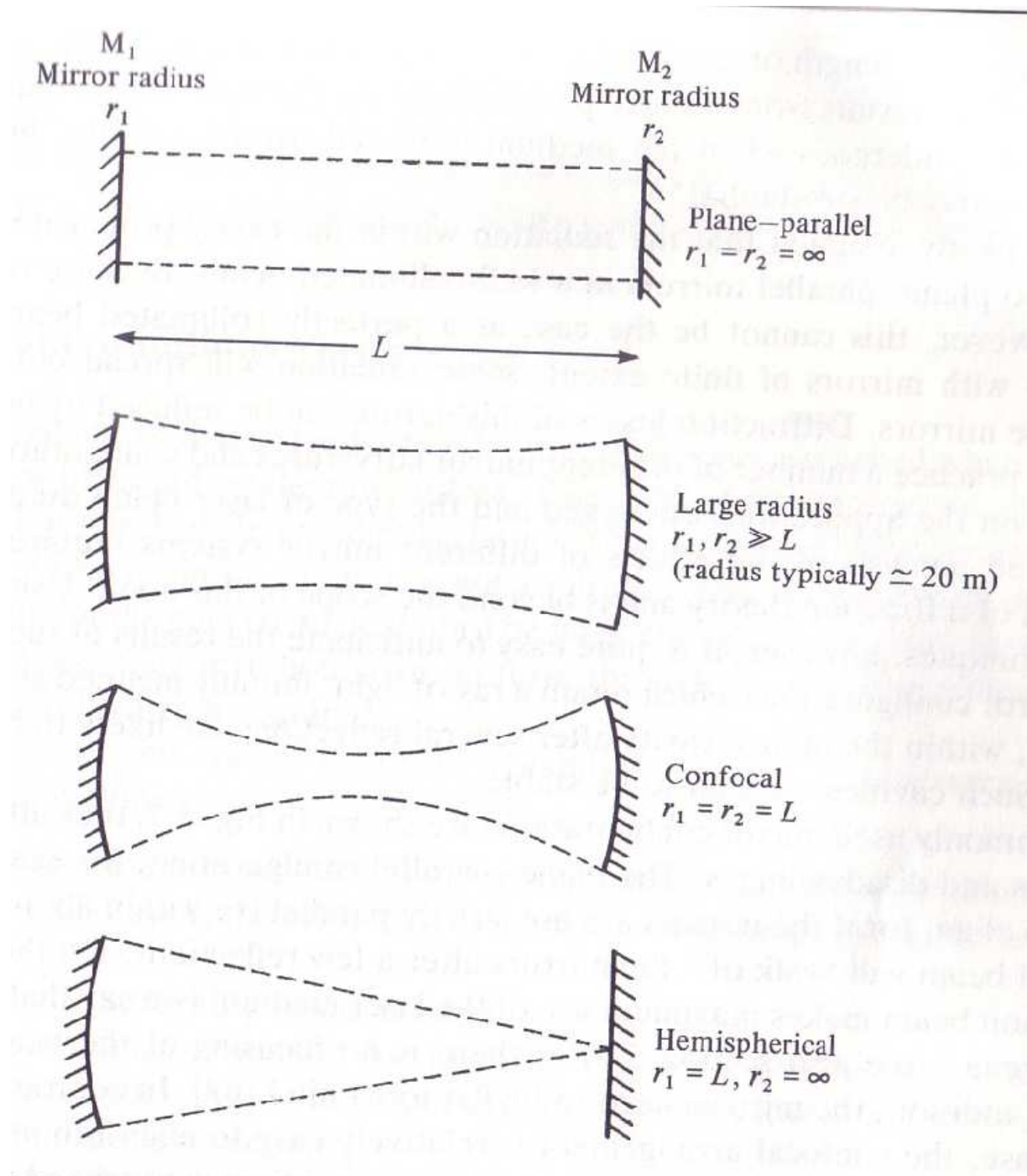


Figure 9: Laser cavity geometries

These are shown in Fig. 9.

In each case one mirror is made highly reflecting while the other is made to leak so that the beam penetrates to the outside world. In many lasers tuning is achieved using filters and/or quarter wave stacks on the mirrors to select specific wavelengths.

The power output is limited by a number of loss mechanisms:

- the transmission of the output mirror
- absorption and scattering at the mirrors
- absorption in the medium from other transitions
- optical scattering in the medium
- diffraction in the cavity

A laser cavity has a characteristic life time. Let the loss (output beam) at one end of the cavity be:

$$\Delta W = -W(1 - R)$$

where W is the energy density and R is the reflectivity.

The time for 1 round trip up and down is:

$$\Delta t = \frac{2L}{v}$$

where L is the length of the cavity and v is the velocity.

So we have the rate of loss of energy density as:

$$\frac{\Delta W}{\Delta t} = -W(1 - R)\frac{v}{2L}$$

Integrating we get:

$$\ln(W) = \ln(W_o) - (1 - R)\frac{vt}{2L}$$

So the time constant of the cavity is:

$$t_c = \frac{2L}{v(1-R)}$$

$$W = W_o \exp\left(\frac{-t}{t_c}\right)$$

If the gain is switched off then the output decays exponentially. This can control the coherence of the output beam.

e.g. $R=0.99$, $L=5\text{mm}$, $t_c \sim 3.3 \text{ ns}$

$$\Delta\nu = \frac{1}{t_c} = 3 \times 10^8 \text{ Hz.}$$

or correlation length:

$$ct_c = 1 \text{ m}$$

So the number of round trips up and down the cavity is ~ 100 .

If the frequency is $3 \times 10^{14} \text{ Hz}$ (optical) then the Q factor is given by:

$$Q = \frac{\nu}{\Delta\nu} \sim 10^6.$$

3.5 Line broadening

So far we have ignored the fact that the spectral lines or transitions have a finite width, they are not truly monochromatic.

The *small signal gain* must be written as:

$$\kappa(\nu_s) = (N_2 - N_1 g_2/g_1) B_{21} h \nu_s n g(\nu_s)/c$$

where $g(\nu)$ is the line profile function and the beam is monochromatic with frequency ν_s .

The shape of $g(\nu)$ arises from the following:

- Doppler broadening - physical motion of the atoms
- collision (pressure) broadening - a third interrupting particle
- natural broadening - the life time or damping of the transition

If all atoms yield the SAME centre frequency then a Lorentzian profile results. This is the case for natural broadening.

$$g(\nu) = \frac{\Delta\nu}{2\pi} \frac{1}{(\nu-\nu_0)^2 + (\Delta\nu/2)^2}$$

If each atom yields a different centre frequency as in the case of Doppler broadening, then a Gaussian profile results.

$$g(\nu) = \frac{2}{\Delta\nu} \sqrt{\ln(2)/\pi} \exp(-\ln(2)(\frac{\nu-\nu_0}{\Delta\nu/2})^2)$$

$$\text{Note } I(\nu, x) = I(\nu, 0) \exp(\kappa(\nu)x)$$

Since $\kappa(\nu) \propto g(\nu)$ we do NOT get the line profile on amplification. The non-linear response boosts the centre frequencies and produces *spectral narrowing*.

Typical transmission and emission profiles for a single transition are shown in Fig. 10.

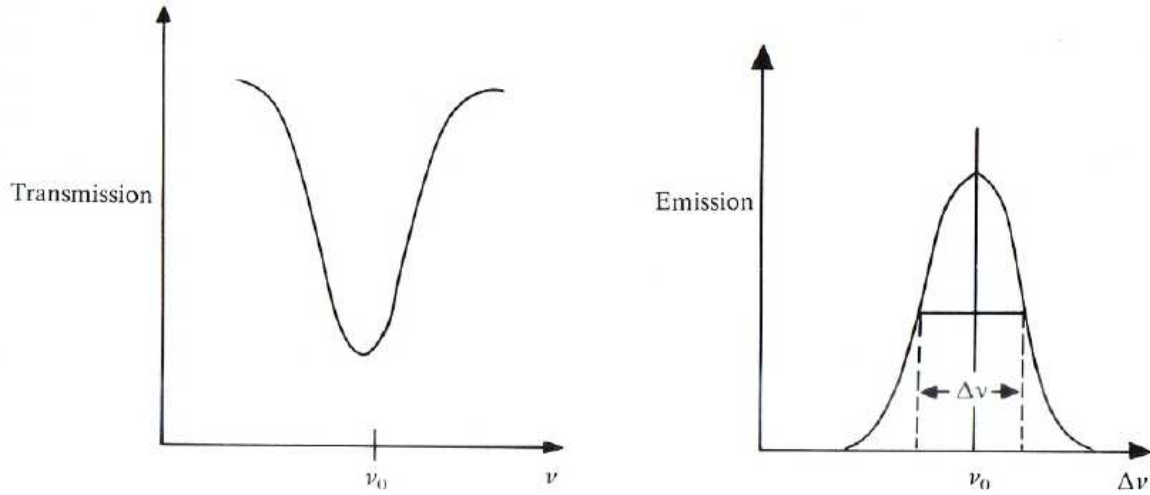


Figure 10: Transition profiles of transmission and emission

3.6 Laser modes

In the resonant cavity formed by the mirrors we get a standing wave pattern of electric field intensity.

We know $p\lambda/2 = l$ where p is an integer and l is the optical path length of the cavity. Therefore we get a series of frequencies given by:

$$\nu_p = pc/2l$$

Each p defines an axial mode of the cavity. The separation of the modes is therefore

$$\delta\nu = c/2l$$

Only those modes which lie within the peak of the gain profile will be amplified and maintained. Note that the peaks are much narrower than the Fabry-Perot resonance response because of the gain.

Fig. 11 illustrates how the combination of the gain profile and cavity modes give rise to a series of closely packed excited modes.

The width of the mode peaks is usually described in terms of a Q factor.

$$Q = \frac{2\pi(\text{energy stored})}{(\text{energy dissipated per cycle})} = \nu / \Delta\nu$$

Typically $Q = 10^8$ which is very large compared with, say, 100 for an electrical oscillator.

The $\Delta\nu \approx 1\text{MHz}$ compared with 10^9Hz for a Fabry-Perot cavity.

If care is taken to reduce losses the Q can be very high.

The electric field vector is always transverse so we get so called TEM's, *transverse electric modes*.

The modes are labelled by the number of minima in the electric field intensity seen when scanning up or across the cavity. So we get TEM_{00} , TEM_{01} etc..

The TEM_{00} mode adjusts itself so that the mirror surfaces are surfaces of constant phase.

The TEM_{00} mode can be selected out using a suitable aperture in the centre of the cavity producing a so called *uniphase mode*.

Fig. 12 shows the intensity distribution of TEM modes at the centre of a laser cavity.

Fig. 13 illustrates the TEM_{00} mode. The value of ω_0 on the diagram is usually defined to be the width of the mode such that the field amplitude has dropped to $1/e$ of its maximum value.

Uniphase operation gives very high spectral purity.

Multimode operation can give high power.

3.7 The hallmarks of laser activity

Laser activity can be distinguished from amplified spontaneous emission, superluminescence or similar phenomena by:

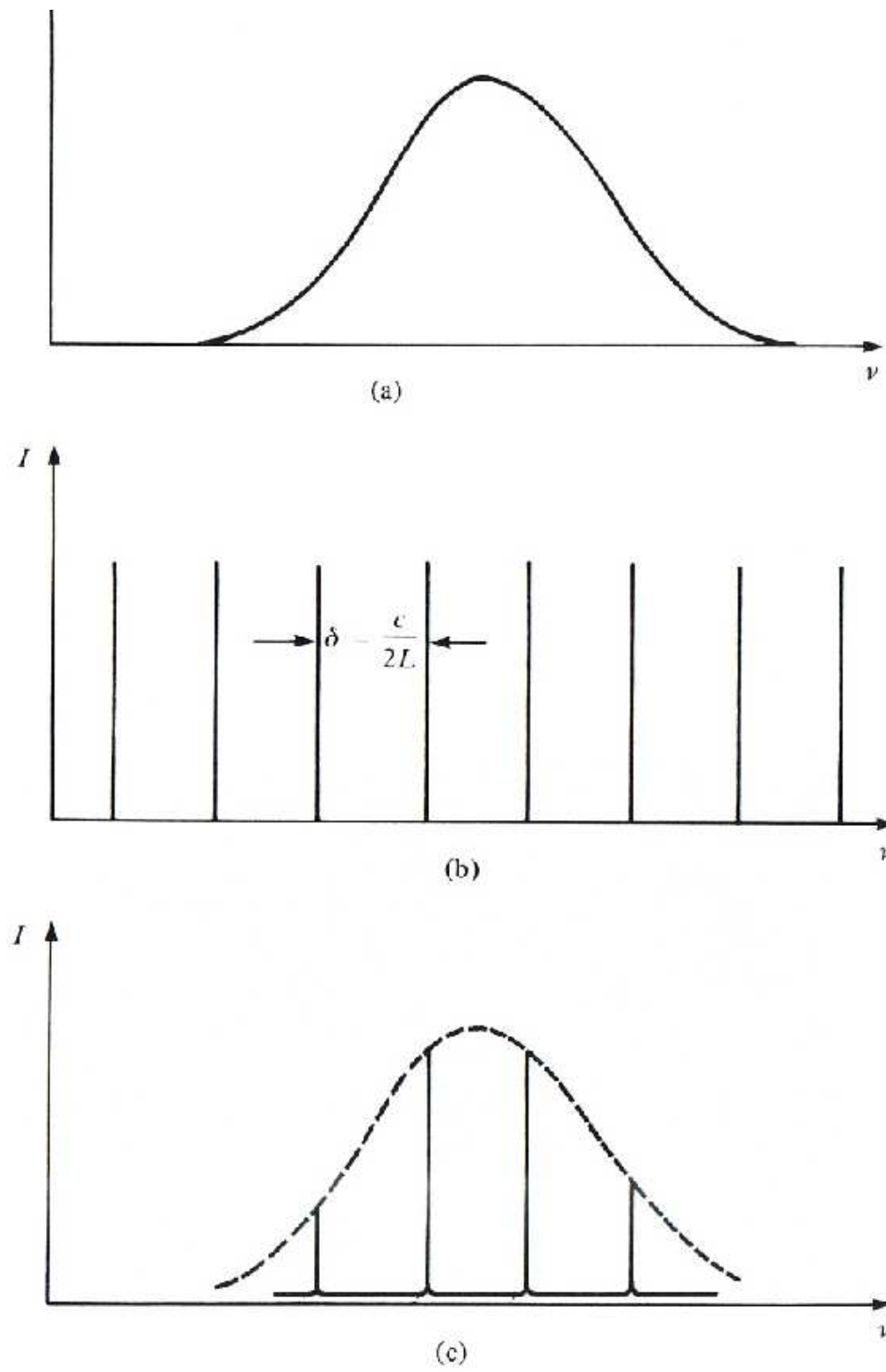


Figure 11: Excited laser modes within the gain profile

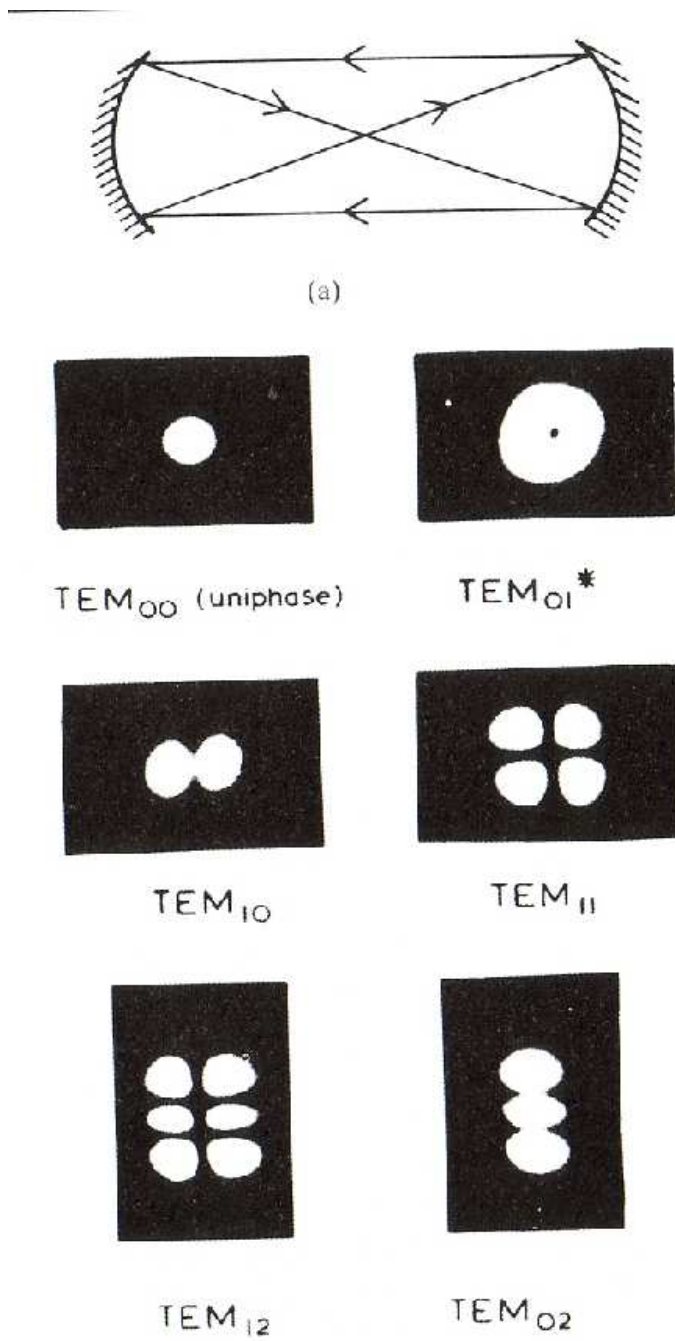


Figure 12: Intensity of TEM modes at centre of laser cavity

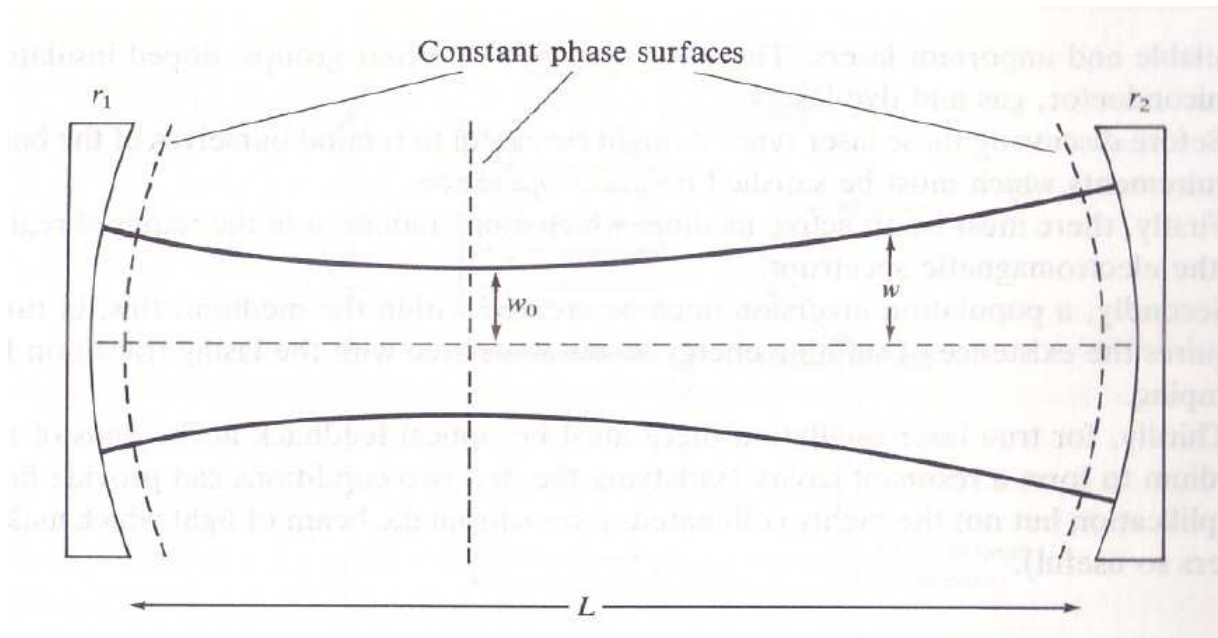


Figure 13: TEM_{00} mode

- A threshold in output energy as a function of input or pumped energy with a high lasing efficiency above the threshold.
- Strong polarization of the output beam.
- Spatial coherence as indicated by a diffraction limited output beam or speckle.
- Significant spectral line narrowing.
- The existence of laser cavity resonances or modes.

4 Types and classes of laser

4.1 Doped insulator lasers

The active medium is solid, usually crystalline, containing impurities often introduced by doping.

Historically this was the first class of laser, using ruby crystals.

A more modern example is Nd:YAG which consists of yttrium aluminium garnet ($Y_3Al_5O_{12}$) with neodymium Nd^{3+} impurity in yttrium sites. It is this impurity which does the work.

Fig. 14 is a simplified energy level diagram of a Nd:YAG system. Essentially a 4 level system with a laser transition of $\lambda = 1.06\mu m$ (1.17eV).

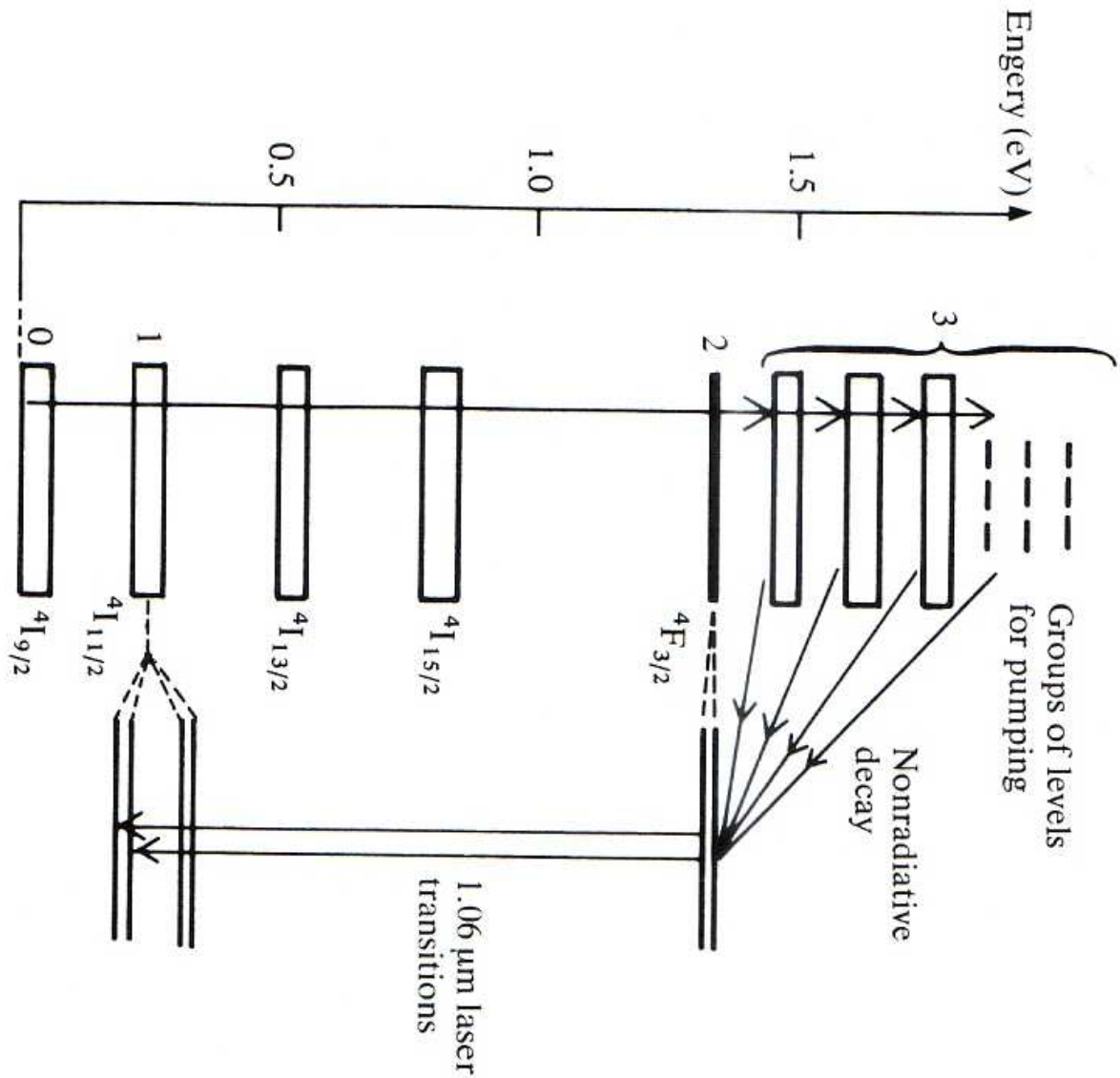


Figure 14: The Nd:YAG energy level diagram

Pumping is by optical flash, using a light pulse of duration 1ms. Fig. 15 shows a schematic of the complete optical system.

The laser starts 0.5ms after the pumping flash starts and the output consists of a series of $1\mu s$ pulses separated by $1\mu s$. This is because the energy loss due to the LASER action is

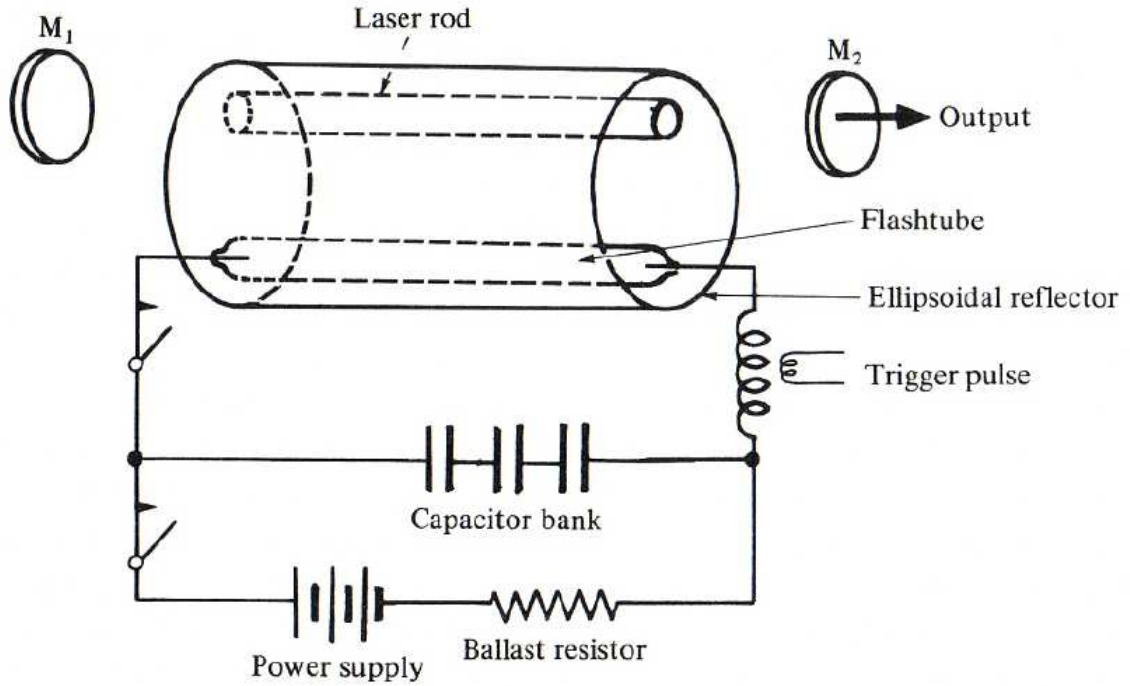


Figure 15: Schematic of the optical system in a doped insulator laser

faster than the pumping. Such pulsing behaviour reduces the coherence of the laser light because the spikes are unrelated.

The efficiency is only about 0.1%. By contrast the related Nd:Glass laser produces 3 times the power of Nd:YAG but has a broader line width.

4.2 Semiconductor lasers

They are basically a diode junction. In order to get LASER action there needs to be a region where BOTH excited electron states and holes (vacant electron states) are present.

This is achieved using heavily doped n and p material and applying a forward bias to the junction. Fig. 16 shows the energy levels either side of the diode junction.

Under forward bias the active region is only thin, for example in GaAs at room temperature 1 to 3 μm . This thickness is controlled by the diffusion length of the electrons. The geometry of the active region is shown in Fig. 17.

No external mirrors are used. The faces are cleaved or ground perpendicular to the

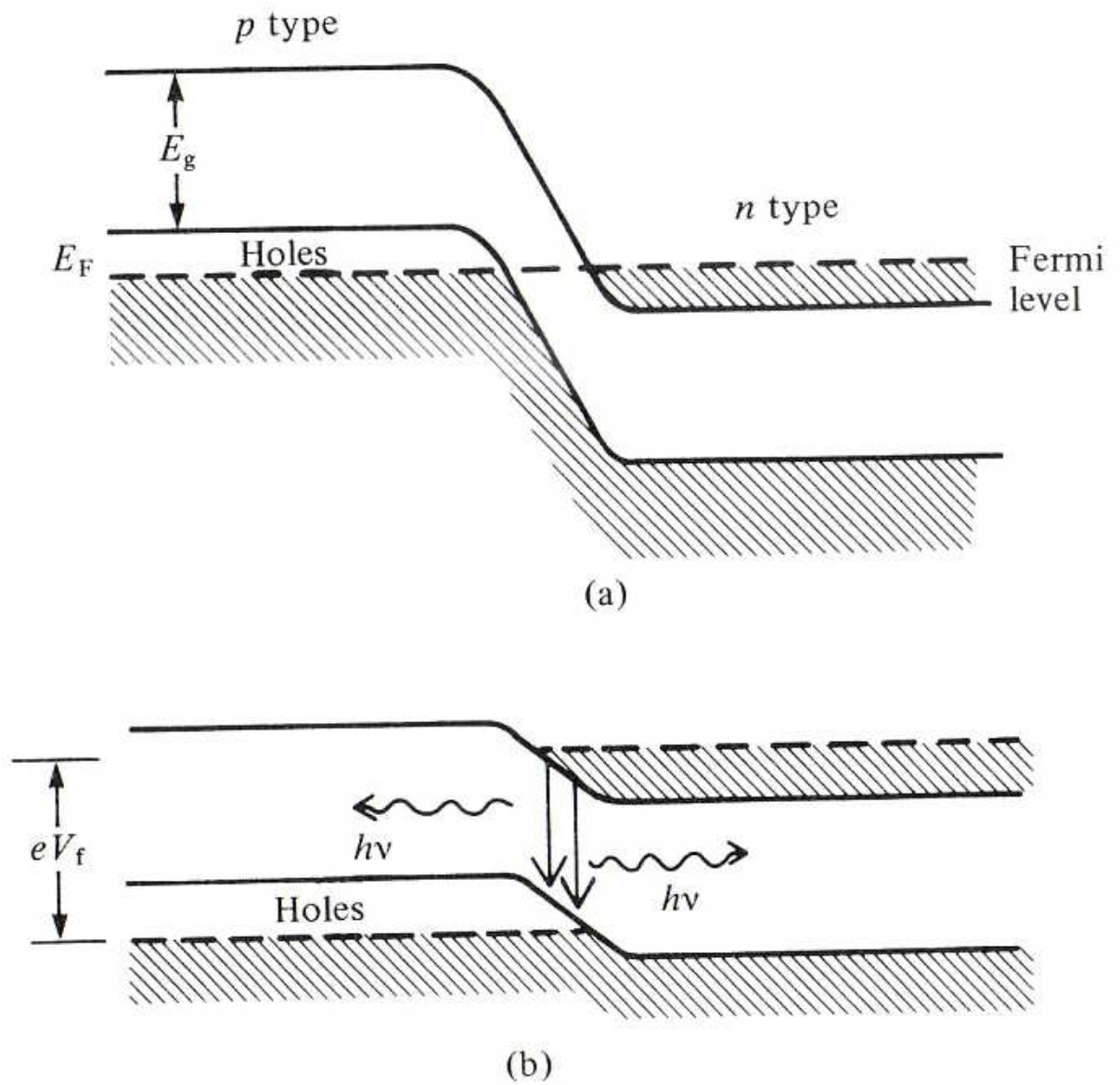


Figure 16: Energy levels in a semiconductor laser (a) in equilibrium and (b) with forward bias

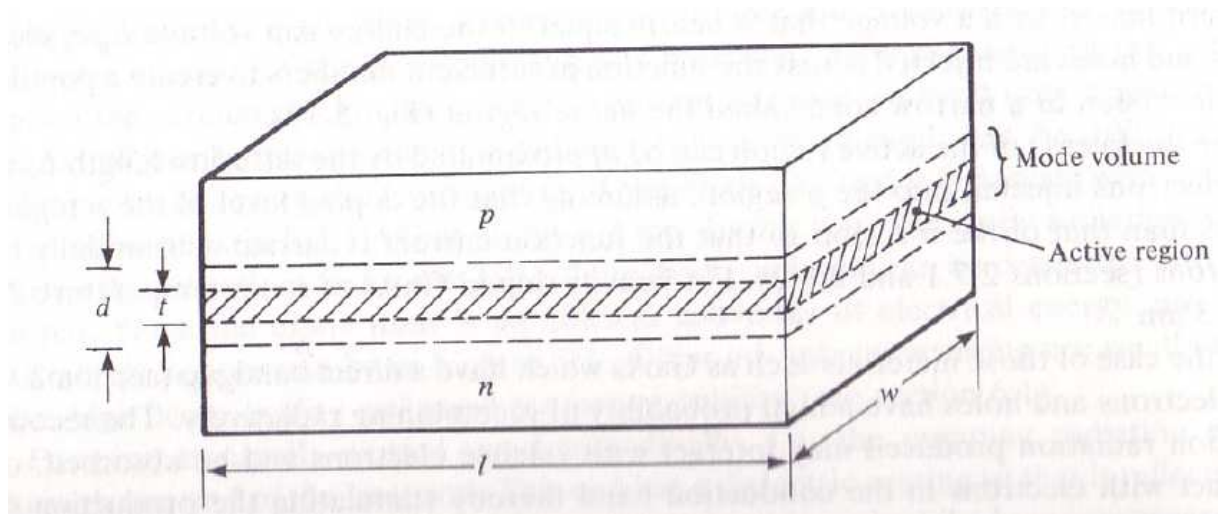


Figure 17: The active region of a semiconductor laser

junction. Using Fresnel's equations the normal incidence reflectivity is determined by the refractive index. For example $n = 3.6$ for GaAs which gives a reflectance of 0.32.

The active junction region has a slightly different n so acts as a waveguide which contains the laser light. A schematic view of the complete semiconductor laser is given in Fig. 18.

The pumping energy comes from the diode current. LASER action is induced above a certain threshold current density.

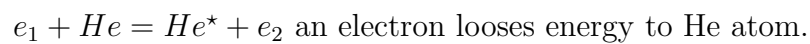
The principle loss mechanism is scattering by optical inhomogeneities in the active volume.

Because the active region is thin the exit beam spreads due to diffraction. The beam fans out perpendicular to the junction plane.

$$\theta = \lambda/t, \text{ if } t = 3\mu m \text{ and } \lambda = 0.84\mu m \text{ then } \theta = 19^\circ.$$

4.3 Atomic gas lasers

The common He-Ne laser. Ne provides the energy levels and He provides pumping by electron and atomic collisions. Pumping is by a two stage process:



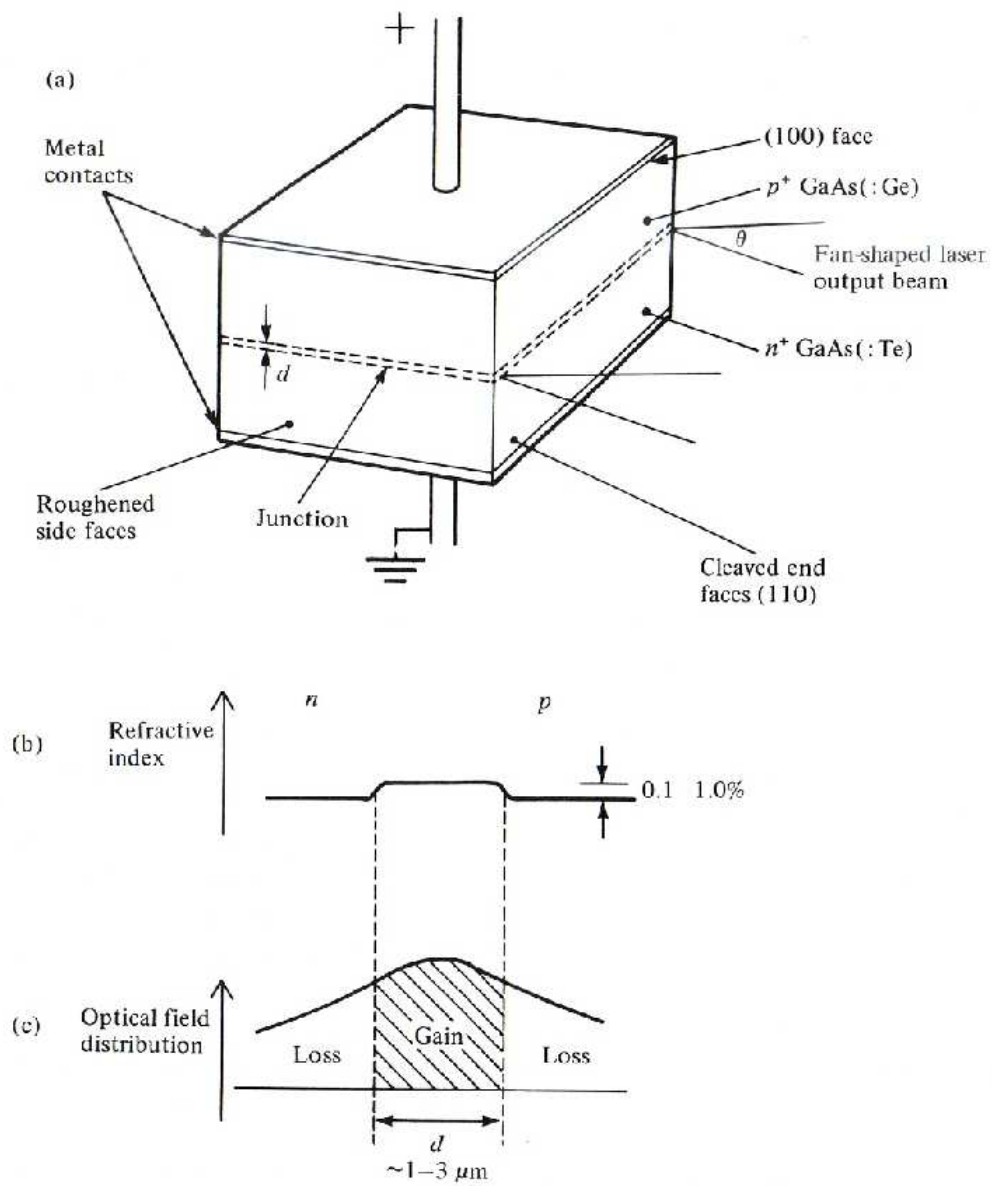


Figure 18: A semiconductor laser

So pumping is by d.c.discharge, 2 to 4 kV across a tube of gas at 10 torr.

A complete system is shown in Fig. 19 and the energy level diagram for the He-Ne laser is shown in Fig. 20.

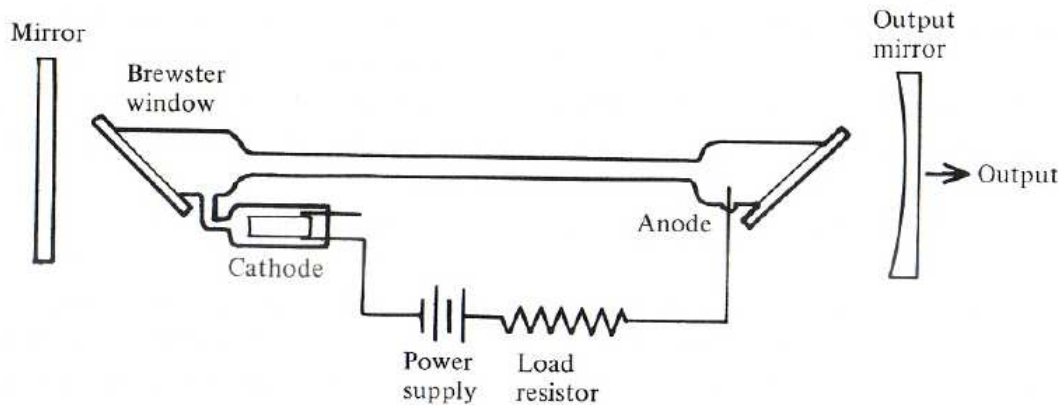


Figure 19: The atomic gas laser

Low power but high collimation, polarization selected by Brewster window and $\Delta\lambda$ extremely small. The Fresnel reflectivities utilized in a Brewster window are shown in Fig. 19.

4.4 Ion lasers

The principle of operation is similar to atomic gas lasers but high discharge currents are used to strip the atoms of electrons to form ions.

An example is the Ar ion laser. Powerful Continuous Wave operation can be achieved by complicated discharge geometry to maximize the pumping power.

Several watts CW output or upto 1 kilowatt in microsecond pulses can be generated.

High discharge current 15-50 A. Pump to 4P states, 35eV above ground state by multiple collisions. Transitions correspond to 4P-4S, 514.5nm and 488nm. Use Brewster window at ends of gas tube to isolate a single polarisation with minimum reflection losses.

The construction of a typical argon ion laser is shown in Fig. 21.

Used to pump dye lasers (see below).

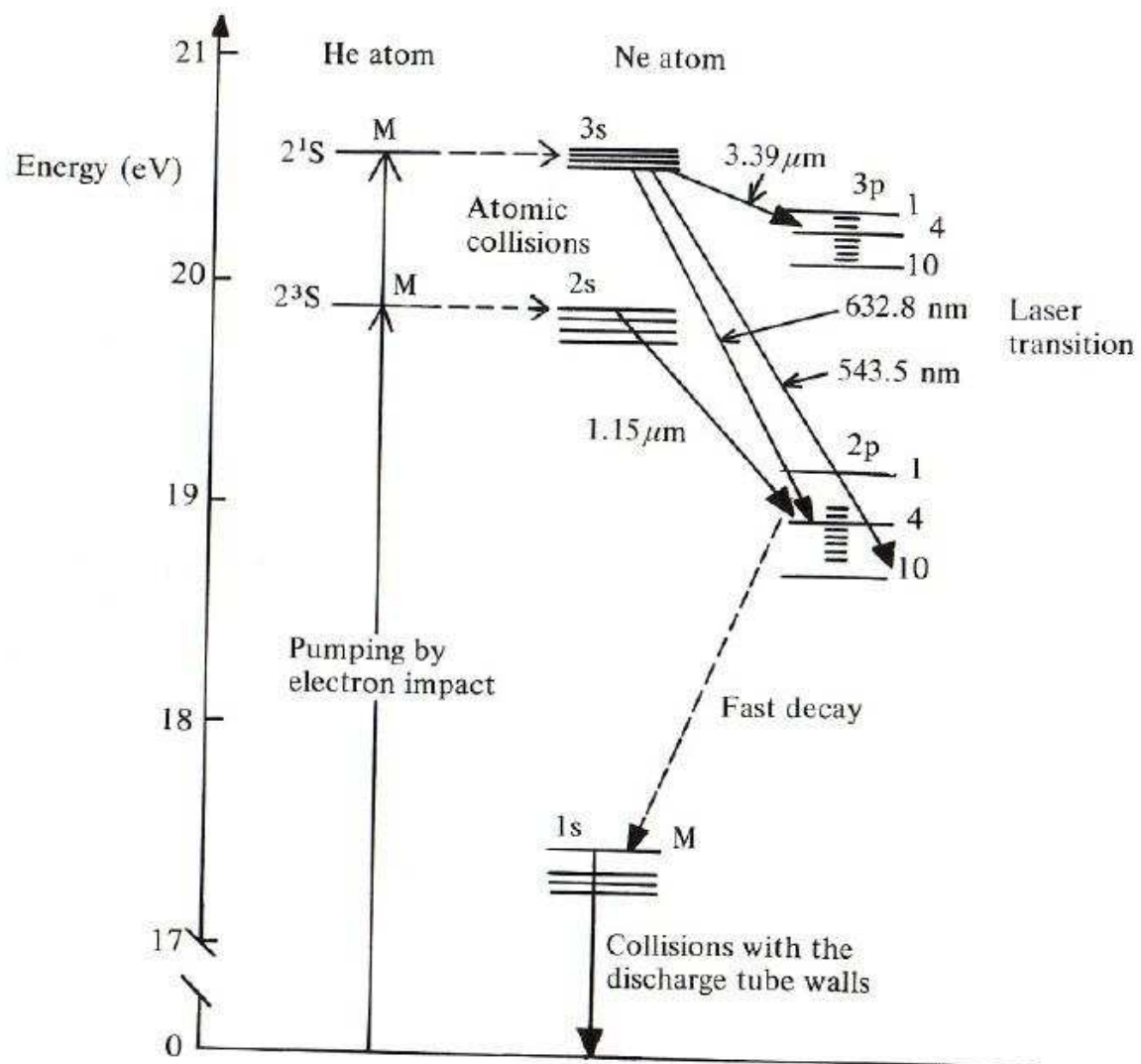


Figure 20: The energy level diagram of the He-Ne laser

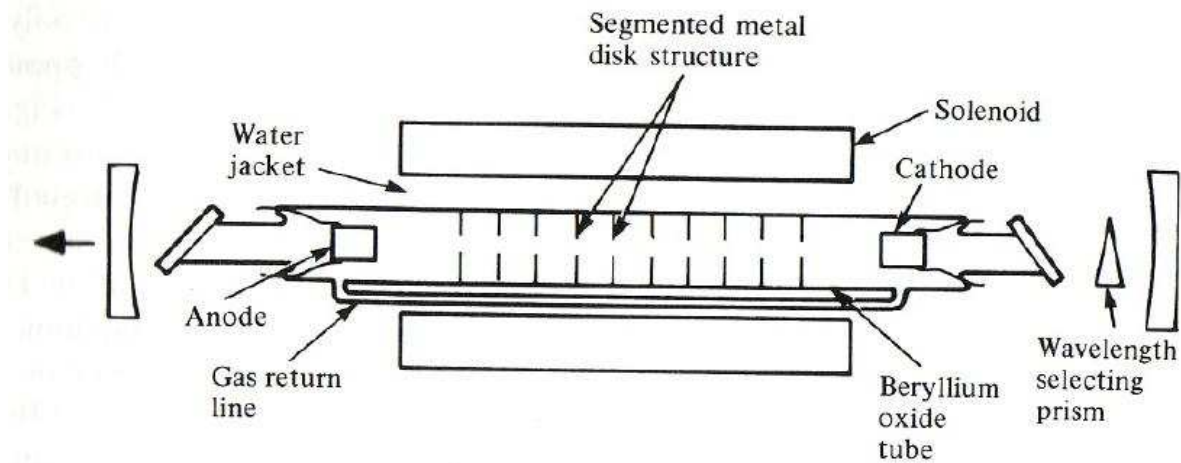


Figure 21: The construction of an argon ion laser

4.5 Molecular lasers- the carbon dioxide laser

Very important in technological and industrial applications.

Use the vibrational modes of the molecule. Get the output in the IR. For CO_2 laser the main transition is at a wavelength of $10.6\mu m$. The vibrational modes of the molecule are shown in Fig. 22 and the energy level diagram for the CO_2 system is shown in Fig. 23.

Again use d.c. discharge to pump but because the coupling between the energy levels is so high this type of laser can be very efficient, upto 30%.

Can easily obtain 100 watts CW from a laser 1 metre long.

Using gas dynamic pumping can get an incredible 100kW of CW power.

Compress and heat a mixture of nitrogen and carbon dioxide. In this state a large amount of energy is stored in vibrational modes of the N_2 . If the gas is then allowed to expand fast into a low pressure region the temperature drops and some energy is transferred by resonant collisions into the (001) state of the CO_2 thus creating a population inversion.

4.6 Liquid dye lasers

These contain an organic dye in a solvent.

Such dyes can be excited by absorption of short wavelengths and fluoresce by emitting at longer wavelengths.

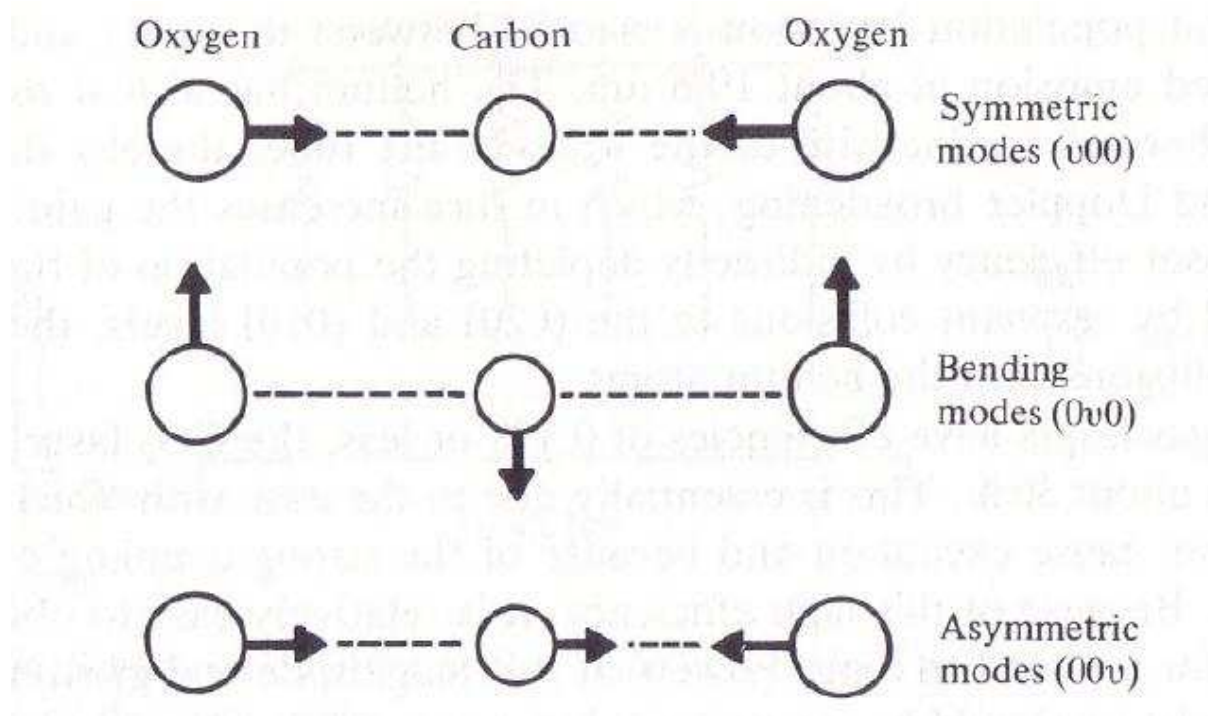


Figure 22: The vibrational modes of a CO_2 molecule

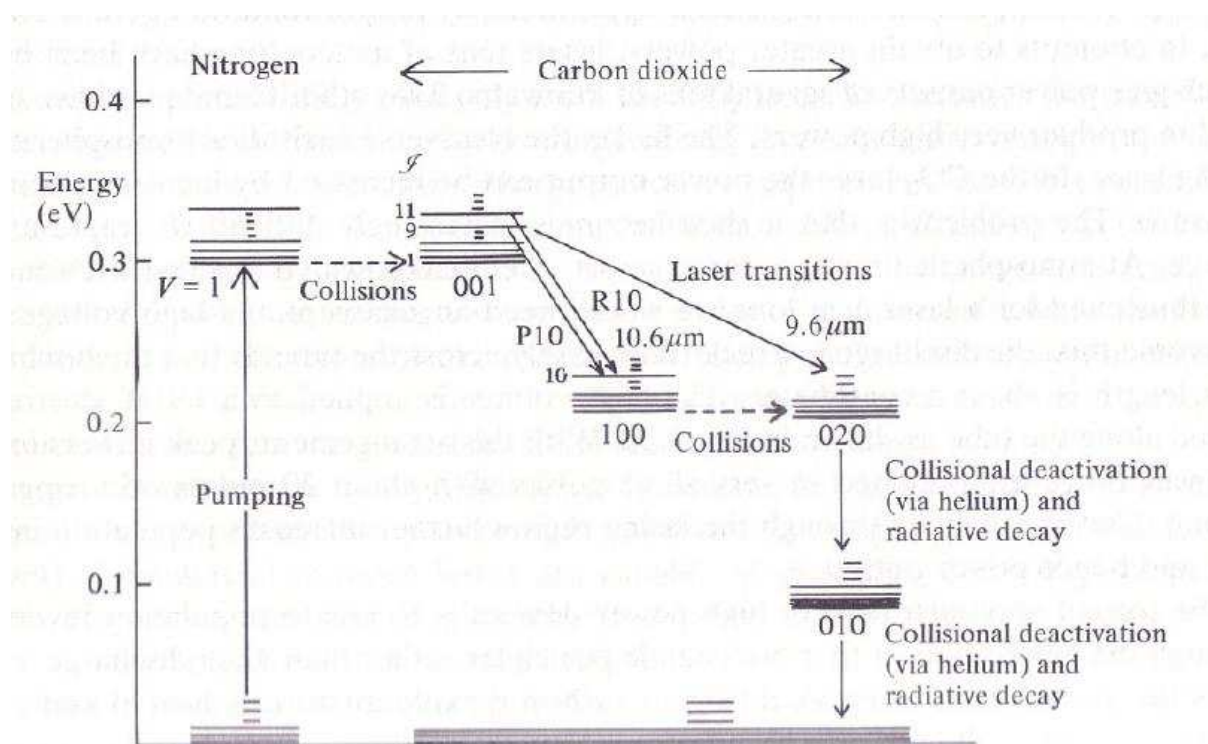


Figure 23: The energy level diagram of a CO_2 laser

There are a large number of electronic energy levels in bands. Therefore get a large number of possible LASER transitions and such lasers are *tunable*.

Pumping is done optically using radiation from another laser, for example a Ar ion laser.

A schematic of the energy level diagram of a liquid dye laser is given in Fig 24. The output spectra from various dyes are shown in Fig. 25. The optical elements of a tunable laminar flow dye laser are shown in Fig 26.

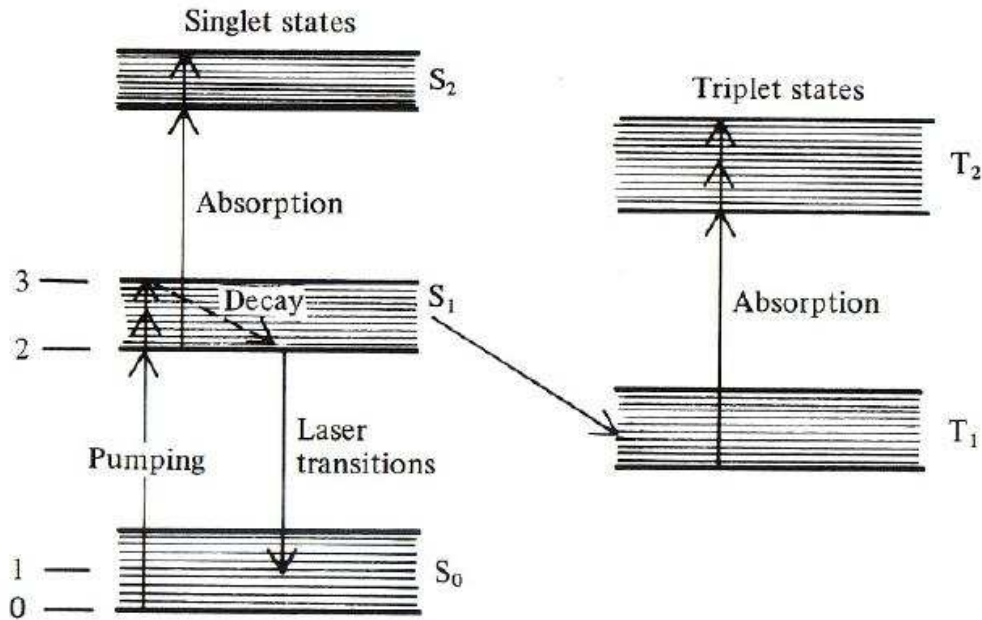


Figure 24: Schematic energy level diagram of a liquid dye laser

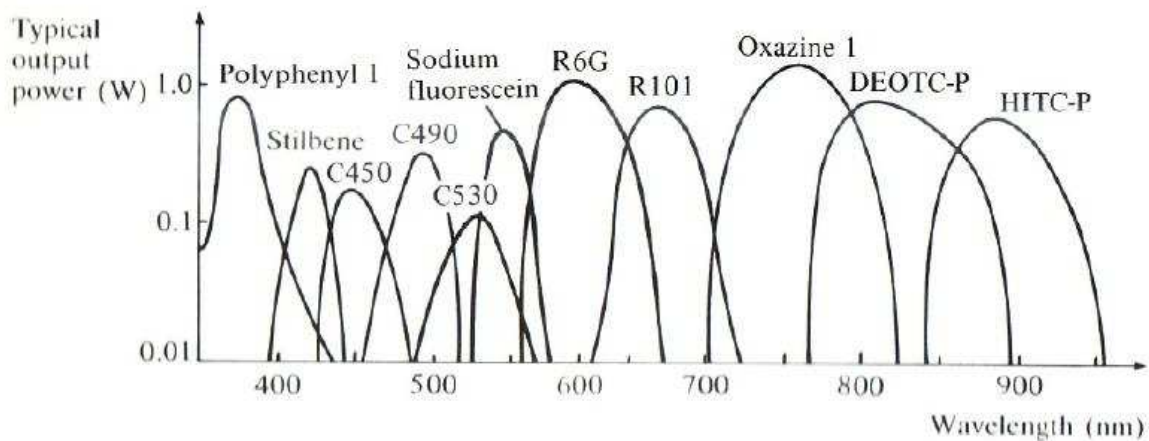


Figure 25: Output spectra from various dyes

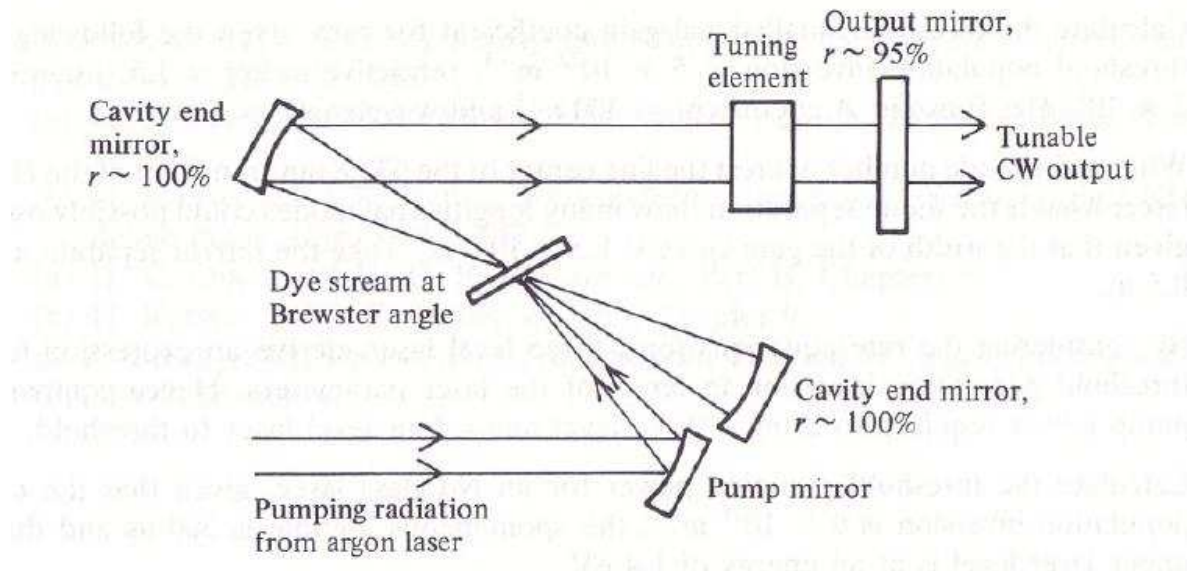


Figure 26: The optical layout of a tunable flow dye laser

Use laminar flow in a thin layer to prevent build up of absorption losses (absorption T1 to T2).

The small signal gain is relatively high because in the liquid (dense) state.

4.7 The free electron laser

Unlike the other types of laser there is no medium which contains bound electrons.

The free electrons are stripped from atoms in an electron gun and accelerated to relativistic velocities.

The beam of electrons is injected through an undulator - a periodic array of magnetic dipoles. An initial radiation field from a seed laser or spontaneous emission in the undulator is amplified by the interaction of the electrons with the electromagnetic radiation field. As the electrons pass through the undulator they are accelerated up and down in the transverse direction by the magnetic field. They move in a sinusoidal path and emit Synchrotron Radiation.

The radiation field grows exponentially and this is accompanied by pronounced longitudinal density bunching of the electrons.

The wavelength of the laser is not limited by specific transition energies but depends on the accelerator energy and the undulator properties. VUV and X-ray wavelengths are

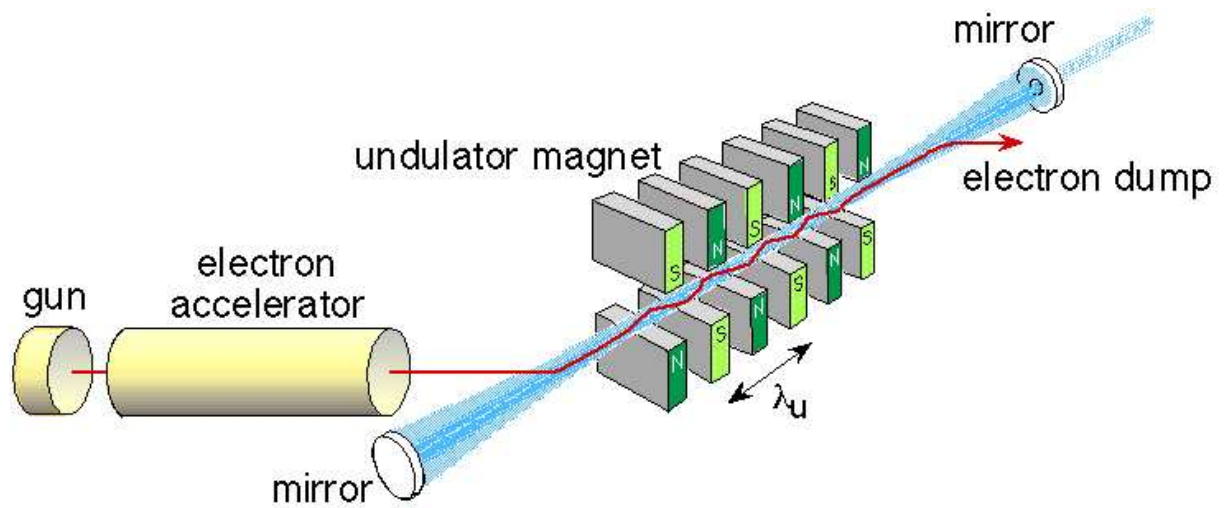


Figure 27: Basic components of a FEL



Figure 28: The undulator at the SRC University of Wisconsin Madison

possible.

Can use mirror cavities in optical but for VUV and X-ray wavelengths mirrors don't reflect at normal incidence and so one pass through a long undulator must be used. In their rest frame the electrons emit dipole radiation but because they are travelling at relativistic velocity the radiation in the laboratory frame is beamed towards the forward direction with open angle:

$$\frac{1}{\gamma} = \frac{m_e c^2}{E_e}$$

The deflection of the electrons from the forward direction is comparable to this opening angle so that the radiation generated by electrons along a period of the undulator, λ_u overlaps (interferes constructively) giving the first harmonic radiation wavelength:

$$\lambda_{ph} = \frac{\lambda_u}{2\gamma^2} (1 + K_{rms}^2)$$

where K_{rms} is the ratio of the average deflection angle of the electrons to the typical opening angle of the synchrotron radiation. If B_u is the rms magnetic field in the undulator:

$$K_{rms} = \frac{e B_u \lambda_u}{2\pi m_e c}$$

The interference condition means that in travelling one period along the undulator the electrons slip one period of the radiation wavelength (because the electromagnetic field moves faster than the electrons).

The electrons interact with their own spontaneous emission. Electrons that are oscillating in phase with the EM wave are retarded while those out of phase are accelerated. This leads to electron bunching which in turn amplifies the EM field and the electrons then radiate in phase with the radiation.

To get exponential amplification of this spontaneous emission you need a very monochromatic electron beam, high electron density, precise magnetic field and many periods in the undulator.

In the beginning, with a bunch of N_e electrons, the spontaneous emission power $\propto N_e$. Later with bunching the power $\propto N_e^2$ and the stimulated process dominates.

The exponential gain is expressed using a gain length L_g . The power increases as:

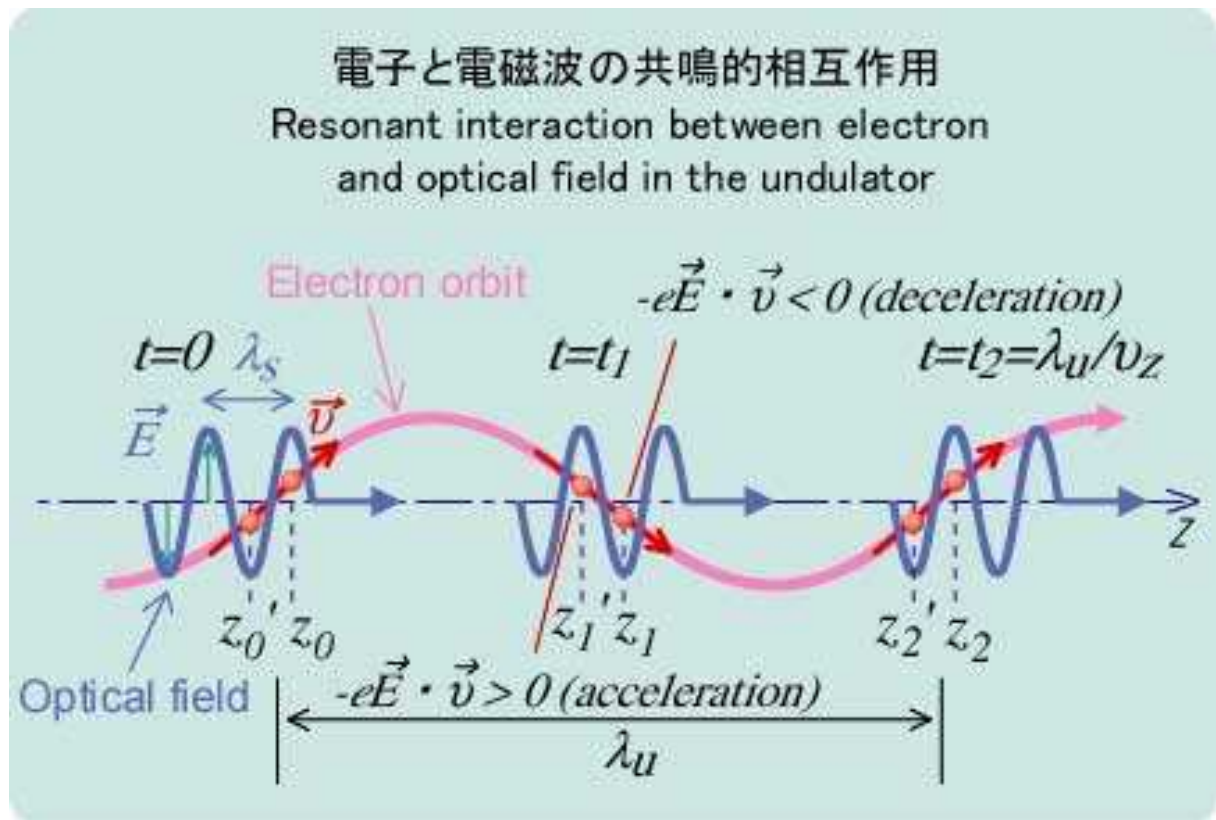


Figure 29: The electron orbit

$$P(x) = P_0 \exp(2x/L_g)$$

where $L_g \approx \lambda_u/(4\pi\rho)$.

$\rho = \Delta\omega/\omega$ is the FEL amplifier bandwidth or ratio of output radiation power to electron beam power. This parameter depends on the quality of the electron beam and undulator and is typically 10^{-3} to 10^{-4} .

The radiation has very high lateral coherence and is plane polarized.

The temporal coherence is limited by the factor ρ above. This is due to the initial shot-noise and the way the electron bunching occurs.

The VUV FEL under construction at the TESLA Test Facility (TTF) at DESY (Deutsches Elektronen-Synchrotron) uses the "self-amplified spontaneous emission" (SASE) mode. It will deliver sub-picosecond radiation pulses with gigawatt peak powers down to a wavelength of 6 nm. So far down to 80 nm.

4.8 The properties of laser light

To greater or lesser extent laser light is:

- very intense
- highly collimated
- highly coherent
- can be continuous or very short pulses

The intensity depends on the pumping power and the efficiency of the LASER mechanism. There is always a tradeoff between the intensity and the coherence and/or collimation.

The collimation is set by diffraction.

$\theta = K\lambda/D$ where $K \approx 1$ and D is the effective aperture diameter.

Typical angular beam widths are:

Type	milli radians
He-Ne	0.5
Ar	0.8
CO ₂	2
Dye	2
Nd:Glass	5
GaAs	20 by 200

The coherence depends on the number of modes excited and the duration of the pulses. Typical coherence values expressed as lengths, L_c , are:

Type	L_c m
He-Ne (single mode)	upto 1000
He-Ne (multimode)	0.2
GaAs	1×10^{-3}
Nd:Glass	2×10^{-4}

5 Photon statistics

When light is detected photons are destroyed. If the detector is sensitive enough then you can count the photons detected - they behave like particles. For example in a photo-multiplier tube each photon generates a cloud of $\sim 10^6$ electrons and if you count these electron clouds (as a current) you can count the photons.

The photon counting statistics, i.e. the probability distribution for the number of photons detected/counted in a given time interval depends on the nature of the light source.

If the source is chaotic, like a light bulb, and the measurement time is much shorter than the coherence time, $t_c = L_c/c$, then the probability distribution is the Planck photon probability distribution (sometimes called the geometric or Thermal distribution):

$$p(n) = \frac{\langle n \rangle^n}{(1 + \langle n \rangle)^{1+n}} \quad (1)$$

where $\langle n \rangle$ is the mean value.

The distribution has variance $(\Delta n)^2 = \langle n \rangle^2 + \langle n \rangle$. The first term on the right-hand side is called the wave contribution and the 2nd term the particle contribution.

If $\langle n \rangle$ is large then we get:

$$p(n) \approx \frac{1}{\langle n \rangle} \exp(-n / \langle n \rangle) \quad (2)$$

and the rms fluctuation is $\Delta n \approx \langle n \rangle$. i.e. the wave contribution dominates if $\langle n \rangle$ is large.

If the measurement time is much longer than the coherence time (or alternatively the measurement time is longer than the characteristic time scale for fluctuations in the source) then the probability distribution is the Poisson distribution:

$$p(n) = \exp(-\langle n \rangle) \frac{\langle n \rangle^n}{n!} \quad (3)$$

which has variance $(\Delta n)^2 = \langle n \rangle$. i.e. we are left with just the photon contribution.

If the light source is coherent, like a laser, then the probability distribution is the Poisson distribution independent of the measurement time.

When a laser starts up the light is initially chaotic but after a few μ seconds it becomes coherent. So the photon statistics measured over very short times changes as the laser light begins.

Measurement of photon statistics is a way of distinguishing between a coherent laser source and a thermal source with a very narrow bandwidth. The 2nd order correlation function, i.e. the probability that photons arrive in coincidence at two photon detectors as a function of the arrival time difference, is used. For a chaotic source the number of coincidences is larger for times below t_c . i.e. the photons have a tendency to arrive in bunches or packets. For coherent light this does not happen. The photon emission from a laser is more regular, without bunching.

6 Optical wave guides - fibre optics

Light can be transmitted from A to B using a transparent dielectric fibre or light pipe.

The principle has been known since 1847 but it is only with the recent development of very thin clad dielectric fibres that light pipes have become useful. So called *fibre optics* now play an important role in communications systems.

The problems that need to be overcome are:

- losses and attenuation
- dispersion
- manufacture
- joining fibres
- injecting and detecting the signal

If the diameter of the fibre is large compared with the wavelength, λ , then the propagation process can be described by geometric (ray) optics.

If the diameter is the same order as λ then we must use wave (physical) optics to describe the behaviour. In this case the fibre acts as a *wave guide*.

Fibre optics utilize Total Internal Reflection (TIR) at the interface between 2 media, where the light is travelling in the denser medium. This is illustrated in fig. 30.

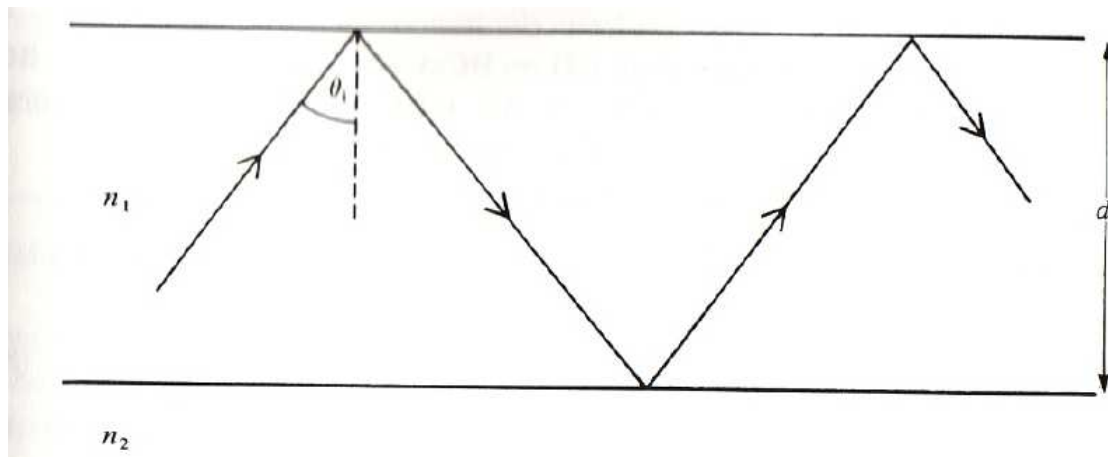


Figure 30: A ray in a planar wave guide $n_1 > n_2$

The critical angle of reflection occurs when $\theta_t = 90^\circ$ and the transmitted ray travels parallel to the surface. Using Snell's law at the critical angle we get:

$\sin \theta_i = n_c/n_f$ where $n_f > n_c$ and the light is incident from n_f .

So the critical angle is given by $\theta_c = \sin^{-1}(n_c/n_f)$

6.1 Planar wave guides - a simple wave model

If the diameter of the fibre, D , is small we must include the effects of interference as the light propagates. To do this we will consider a simple planar waveguide like a microscope slide.

A plane wave is propagating at reflection angle θ_r down a planar guide of width d . Points A and C lie on a common wavefront of all the components travelling in the direction A to B. See fig. 31.

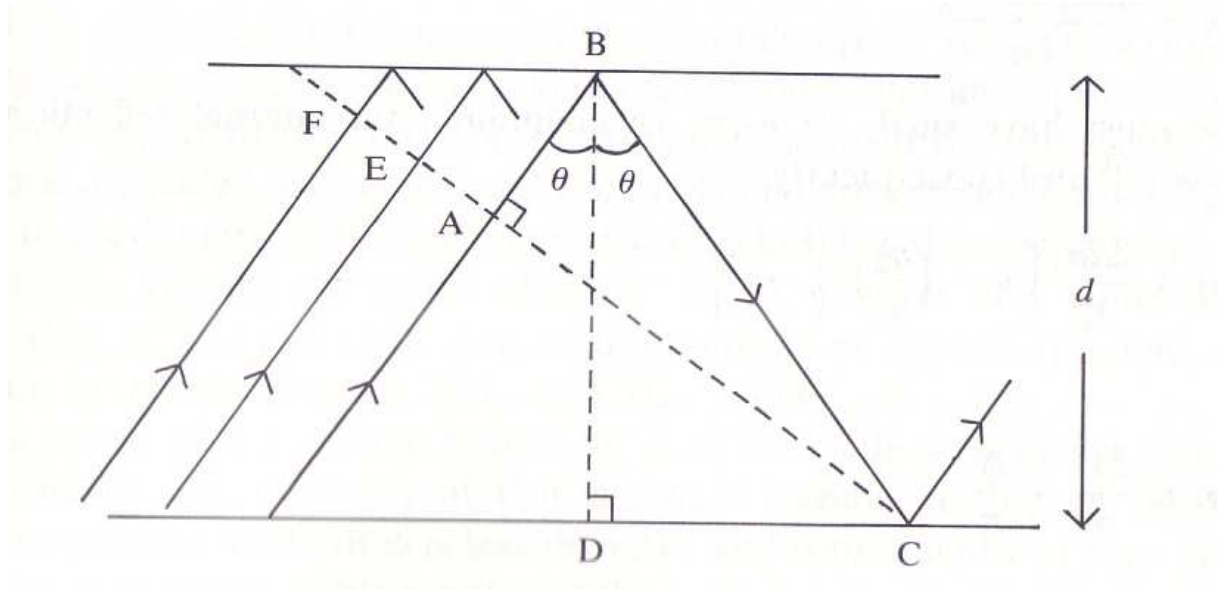


Figure 31: The interference condition in a planar waveguide

The phase difference introduced by reflection A to B to C must be 2π if we are to achieve propagation. Under this condition all the reflected wavefronts interfere constructively.

$(AB + BC)2\pi n_f/\lambda_o - 2\phi = 2\pi m$ where m is an integer and ϕ is the phase change suffered at each reflection.

$$AB + BC = BC(\cos 2\theta_r + 1) = 2BC \cos^2 \theta_r = 2D \cos \theta_r$$

Therefore we get propagation if:

$$2\pi n_f D \cos \theta_r / \lambda_o - \phi = \pi m$$

Unfortunately $\phi = f(\theta_r)$ so we can't solve this equation easily.

However rearranging gives:

$$m = 2Dn_f \cos \theta_m / \lambda_o - \phi / \pi$$

where θ_m is the reflection angle for the m th mode.

But since we have TIR $\sin \theta_m > n_c/n_f$ or

$$\cos \theta_m < \sqrt{1 - (n_c/n_f)^2} \text{ so}$$

$$m \leq (2Dn_f/\lambda_o) \sqrt{1 - (n_c/n_f)^2} - \phi/\pi$$

Since $\phi \leq \pi$ we can estimate the maximum number of modes that can propagate in the wave guide.

If we define $V = (\pi D/\lambda_o) \sqrt{n_f^2 - n_c^2}$ then

$$m \leq (2V - \phi)/\pi$$

V is called the normalised thickness of the film. If $2V < \phi$ then there is no propagation. If $0 \leq (2V - \phi)/\pi < 1$ get just one mode that can propagate.

As you might expect, the larger the normalised thickness V , the greater the number of modes which can propagate.

Fig. 32 shows a ray injected into the end face of the waveguide. In Fig. 32 if $\theta < \theta_c$ then

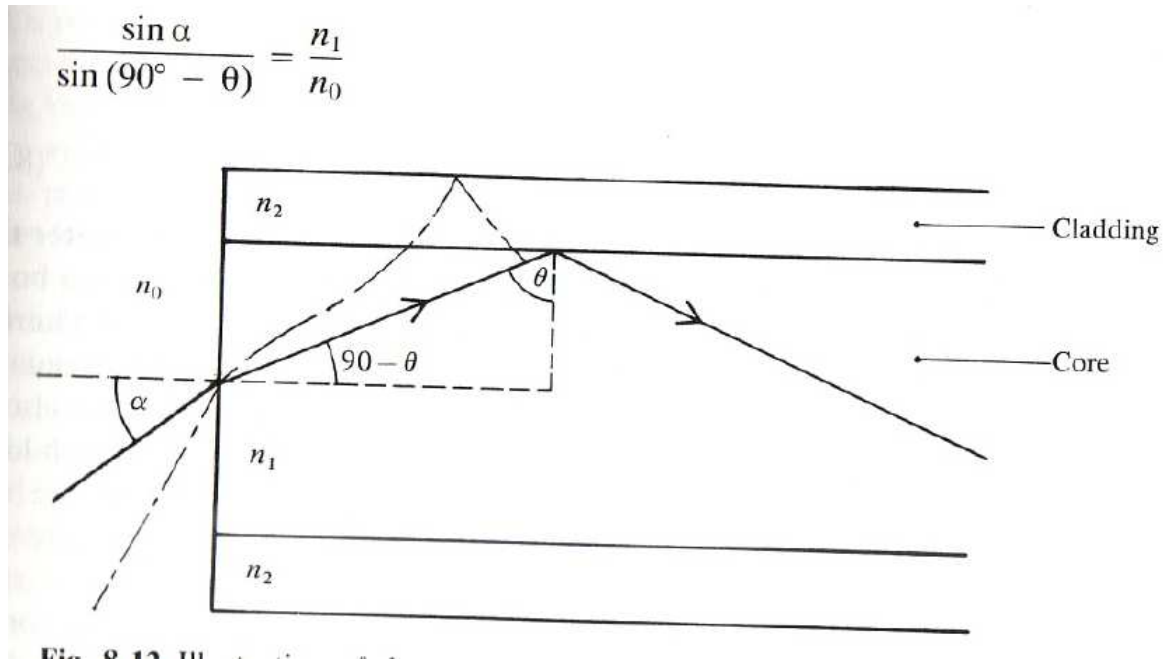


Figure 32: Injection of a ray into the waveguide. α is the injection angle.

we get no TIR and hence no propogation. This defines an α_{imax} .

$$\sin \theta_c = n_c/n_f == \cos(90 - \theta) = \sqrt{1 - \sin^2(90 - \theta)}$$

But from Snell's law $\sin(90 - \theta) = n_o \sin \alpha / n_f$ so

$$(n_c/n_f)^2 = 1 - (n_o/n_f)^2 \sin^2 \alpha_{imax} \text{ or}$$

$$n_o \sin \alpha_{imax} = \sqrt{n_f^2 - n_c^2}$$

$n_o \sin \alpha_{imax}$ is called the numerical aperture. It determines the *speed* or *light gathering power* of the system.

6.2 The uncertainty principle

The argument above shows that light will not propogate down a wave guide if the thickness (or more strictly the normalised thickness) is too small. From the quantum mechanical viewpoint this says that photons will not propogate in the guide if the dimensions are too small. Why not?

Using the de Broglie relationship the momentum of a photon is:

$$P = \frac{hn_f}{\lambda_o}$$

At the limit when $m = 1$ and $\cos \theta_m = \sqrt{1 - (n_c/n_f)^2}$ we get

$$1 \leq \frac{DP}{h} 2 \cos \theta_m - \frac{\phi}{\pi}$$

But $P \cos \theta_m = P_y$ is the transverse component of the momentum and $D = \Delta y$ is the uncertainty in the position of a photon across the guide so we only get propogation if:

$$\Delta y P_y \geq (1 + \frac{\phi}{\pi}) \frac{h}{2}$$

The photons obey the Uncertainty Principle.

6.3 Polarization states

We must consider two polarization states when calculating values of θ_m . If the E vector is in the plane of reflection we get *transverse magnetic* (TM) modes and if H is in the plane

of reflection we get *transverse electric* (TE) modes. The phase change at TIR depends on the polarization state and therefore the propagation angles are different for the TM and TE modes. The mode number m is usually incorporated into the nomenclature so we get TM_m etc..

The electric field amplitude at some position in the guide can be calculated by summing the components reflected from each interface. The effective amplitude in the guide is given by:

$2E_o \cos(\pi m/2 - (\pi m + \phi)y/D)$ where y is the distance from the centre line and D is the width of the guide.

Each mode produces a standing wave pattern across the guide.

When we have TIR at a dense to rare interface there is still field penetration into the rare medium. We get an *evanescent wave* which decays exponentially:

$$E(y) = E_o \exp(-(2\pi n_c y/\lambda_o) \sqrt{n_f^2 \sin^2 \theta_r/n_c^2 - 1})$$

where θ_r is the reflection angle. This expression tells us how thick the cladding must be to give a good reflection.

The electric field amplitudes across the guide are illustrated in Fig. 33.

The path lengths of rays associated with each mode depends on θ_m and so different modes travel at different velocities. This gives rise to *inter-modal dispersion*. The paths are illustrated in fig. 34.

We can calculate the time delay between the extreme modes corresponding to $\theta_{min} = \theta_c$ (m large) and $\theta_{max} = 90^\circ$ (m small).

The velocity is $c \sin \theta/n_f$ so

$$\Delta t = (1/\sin \theta_c - 1/\sin 90^\circ) L n_f / c$$

$$\Delta t = (n_f - n_c) L n_f / (c n_c)$$

To minimize the effects of this delay we must reduce the number of modes. We can reduce D so we get just a small number of possible modes.

The above *ray model* only gives us a qualitative picture of what is happening. If we go the whole way and solve Maxwell's equations for the EM fields in the guide we find that the mode field varies as:

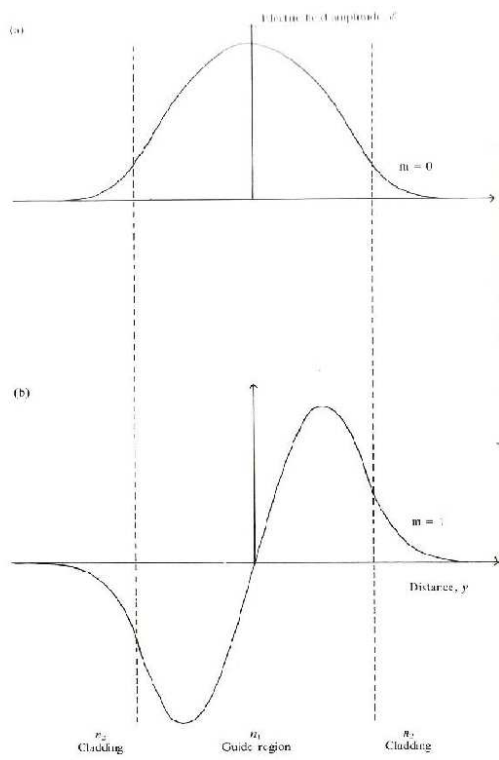
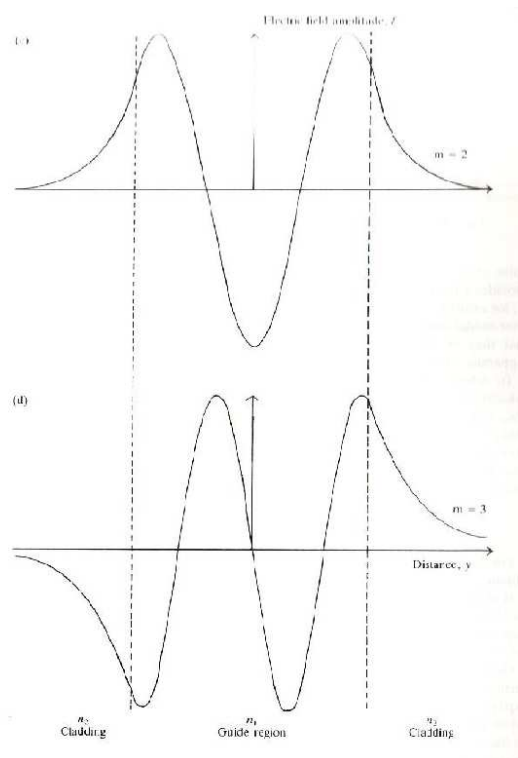


Figure 33: Electric field profiles across a planar waveguide



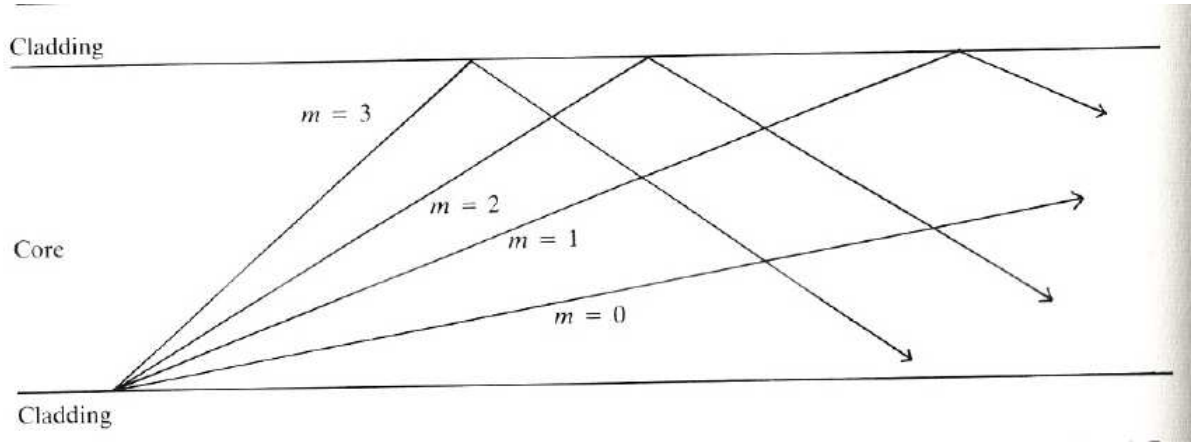


Figure 34: Paths for different modes in a planar waveguide

$\exp i(\omega t - \beta z)$ where z is the axis along the centre of the guide and β is known as the *mode propagation constant*.

You should recall that for such a wave the *phase velocity* is given by ω/β and the *group velocity* is given by $\partial\omega/\partial\beta$.

The phase and group velocity are plotted as a function of β in fig. 35.

Note as we approach θ_c (mode m maximum) the phase velocity is given by c/n_c and as we approach $\theta = 90$ (mode $m=0$) the phase velocity is given by c/n_f .

6.4 Rays in a cylindrical cladded fibre

A cladded fibre has a core refractive index n_f and an outer cladding refractive index n_c which is slightly less than the core. Then rays travelling down the fibre nearly parallel to the axis will suffer TIR.

Consider a meridional ray in the fibre. Such a ray is coplanar with the axis of the cylinder as shown in Fig. 36.

If θ_i is the injection angle wrt the axis and θ_t is the transmission angle wrt the axis inside the fibre then over a fibre length L the path length is given by:

$$l = L / \cos \theta_t = L / \sqrt{1 - \sin^2 \theta_t}$$

The number of reflections in length L with diameter D is:

$$N \approx l / (D / \sin \theta_t) \text{ to within } \pm 1$$

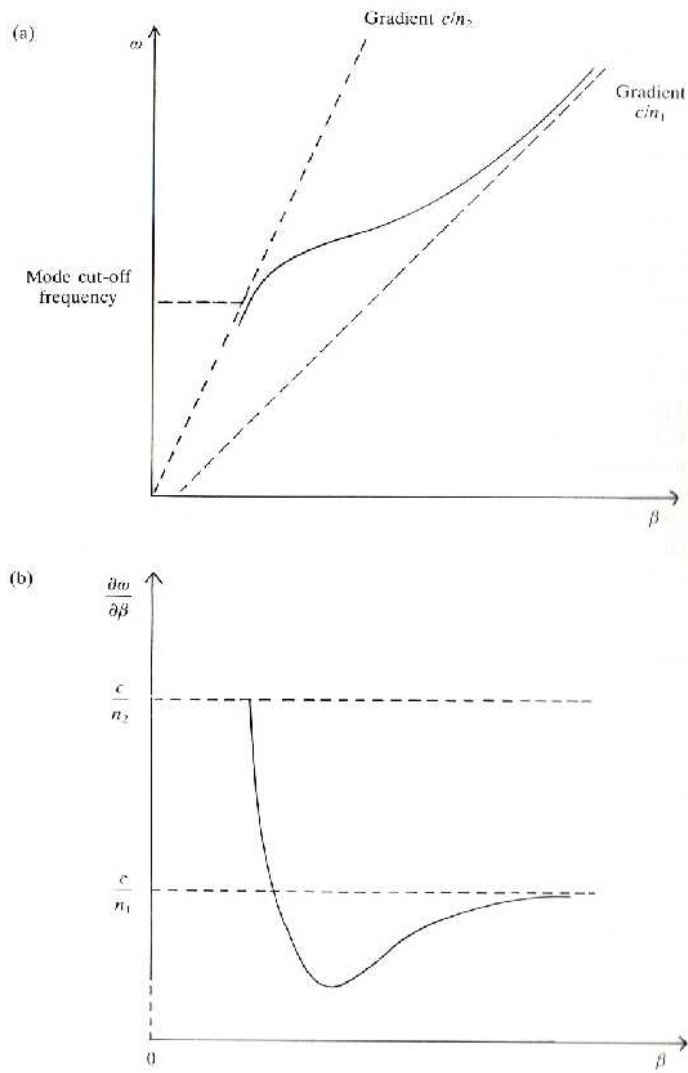


Figure 35: Phase and group velocity

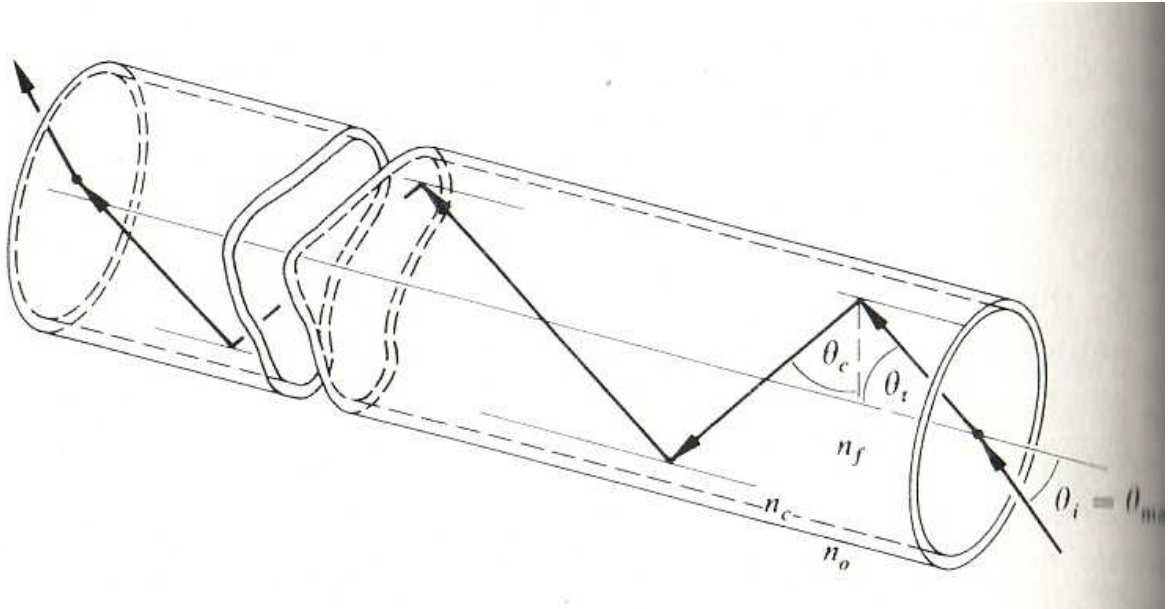


Figure 36: Meridional ray in cylindrical fibre

So if $D = 50\mu m$ and $\theta_t = 30^\circ$, $N=11500$ per metre. Therefore there are potentially a large number of reflections and possible large losses due to imperfections in the surface.

6.5 Fibre optics

A practical fibre optic consists of a very thin core of doped silica (very pure glass) surrounded by a cladding of silica with slightly smaller refractive index. This is then encased in protective coatings of silicone and buffer materials.

To find the modes of propagation in the fibre we should solve Maxwell's equations in cylindrical polar coordinates with the appropriate boundary conditions at the core cladding interface. It is found that there are TM and TE modes similar to the planar waveguide case but 2 integers are now required to label the modes, TE_{ml} . Such transverse modes correspond to meridional rays. However we can also get skew rays which spiral down the cylindrical core and these lead to HE and EH modes in which both E and H have transverse components. The ray picture of these modes is illustrated in Fig. 37.

These modes can be approximated by linearly polarized modes with radial and azimuthal structure in the fibre. These are designated LP_{lm} where the first subscript refers to the azimuthal state and the second to the radial state. The simplest mode has no azimuthal structure LP_{01} . The intensity of modes across the fibre are illustrated in Fig. 38.

We can define a *normalised thickness* for a cylindrical fibre

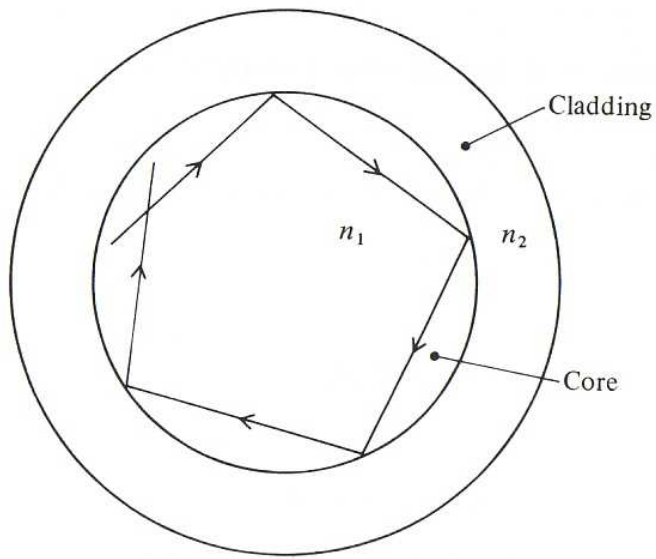


Figure 37: Skew ray in cylindrical fibre

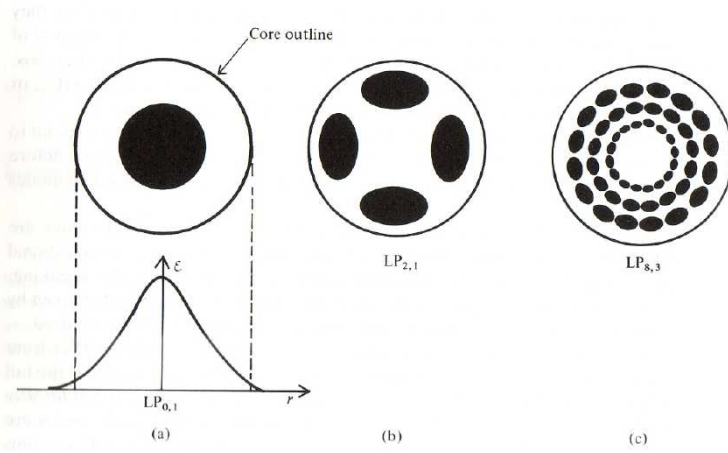


Figure 38: Modes patterns in cylindrical fibre

$$V = (2\pi a/\lambda_o)\sqrt{n_f^2 - n_c^2} = (2\pi a/\lambda_o)(N.A.)$$

where a is the radius of the core and N.A. is the numerical aperture.

If $V < 2.4$ then only the LP_{01} mode can propagate and we get a *single mode fibre*.

$$a < (2.4\lambda_o/2\pi n)/(N.A.)$$

For example if $n_f = 1.53$ and $n_c = 1.5$ if $\lambda_o = 1\mu m$ then $a < 1.27\mu m$. Single mode fibres are very thin!

Thicker fibres that can propagate many modes are called *multimode fibres*. The total number of modes $N \approx V^2/2$ (note now proportional to V^2 because the fibre is cylindrical rather than planar). The crosssections of different types of fibre are shown in Fig. 39.

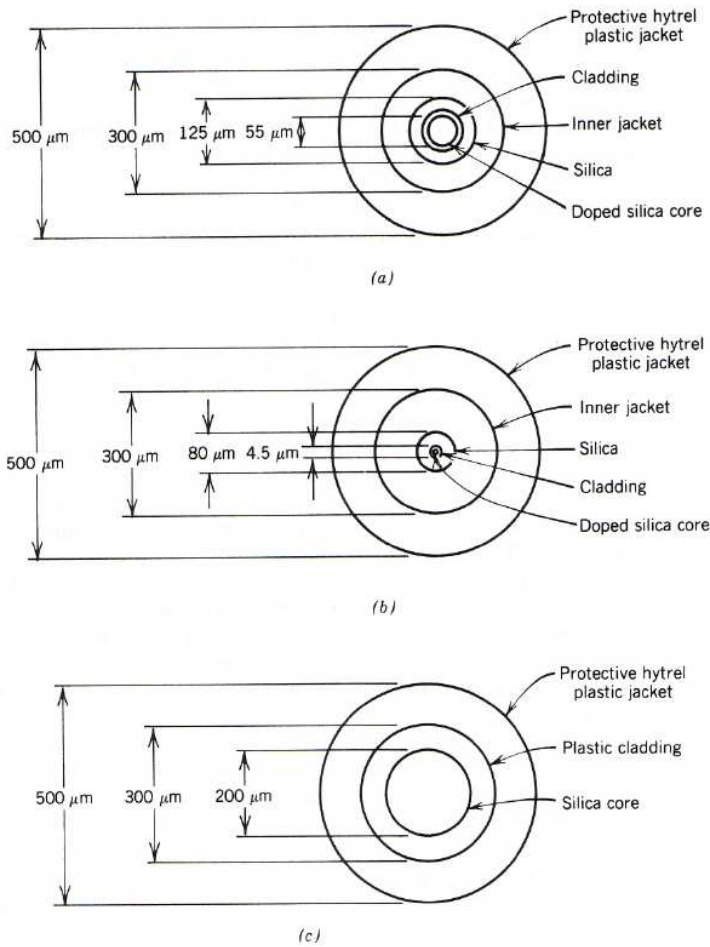


Figure 39: Construction of optical fibres a) Wide-band graded-index multimode, b) Step-index single-mode and c) large-core plastic-clad optical.

6.6 Step index and graded index fibres

In a step index fibre the transition from core fibre index n_f to cladding index n_c is sharp.

In a graded index fibre the core fibre index n_f varies radially through the core with a peak on the axis and a smooth or graded drop to the cladding n_c at the core radius a .

These are illustrated in Fig. 40.

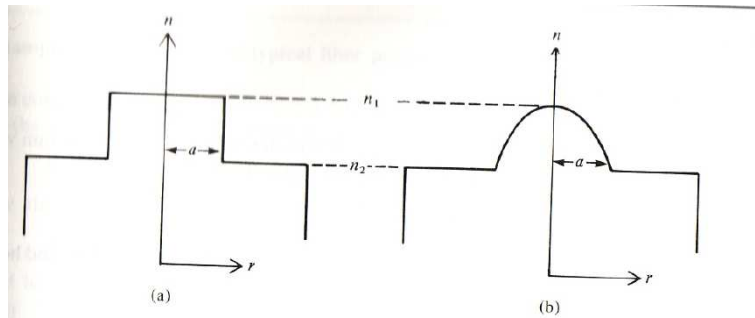


Figure 40: The index profiles of step index and graded index fibres

Both types of fibre propagate 3 kinds of rays:

- central
- meridional
- helical or skew

These are illustrated in Fig. 41.

In a step index fibres the meridional and helical rays have larger optical path lengths and hence are much slower than the central ray mode.

In a graded index fibre the meridional and helical rays (modes) spend less time in regions of high index. Therefore despite the longer physical path length the corresponding modes tend to have velocities which are larger and closer to the central ray mode. That is graded index fibres exhibit reduced intermodal dispersion.

6.7 Dispersion in fibre optics

- intermodal

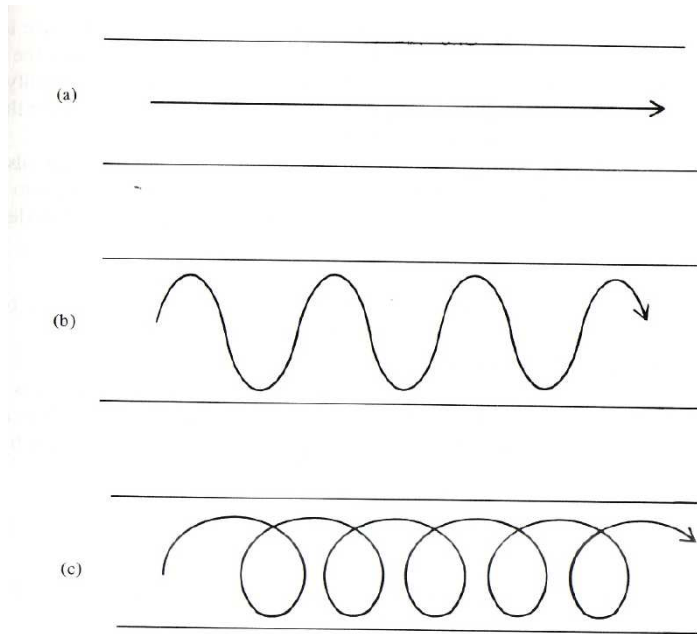


Figure 41: Types of ray in cylindrical fibres

- profile
- material
- wave guide

Intermodal dispersion arises from the different path lengths for propagation modes.

Profile dispersion arises from the fact that $\Delta = (n_f - n_c)/n_f$ is a function of λ . Real sources of light always have a finite bandwidth and so Δ varies over the bandwidth of the pulse. This dispersion depends on both n_c and n_f .

Material dispersion arises because n_f depends on λ so even if the wave is confined to the core we still suffer dispersion from the finite bandwidth.

$$v_g = d\omega/dk = -\lambda^2 dv/d\lambda \text{ but}$$

$$v = c/(\lambda n) \text{ so}$$

$$v_g = (1 + (\lambda/n)dn/d\lambda)c/n$$

If there is a spread of wavelengths $\Delta\lambda$ then the corresponding spread in group velocity will be

$$\Delta v_g = \Delta\lambda dv_g/d\lambda$$

So if we initially have a very short pulse after a distance L it will be spread in time by

$$\Delta t = L(1/v_1 - 1/v_2) = -L\Delta v_g/v_g^2$$

Substituting for v_g and Δv_g gives us an expression for this time delay. In practice the 2nd derivative term $d^2n/d\lambda^2$ dominates and we find

$$\Delta t \approx |-(L\lambda\Delta\lambda/c)(d^2n/d\lambda^2)|$$

For silica this passes through zero for $\lambda = 1.3\mu m$ Fig. 42 shows the 2nd derivative term for silica.

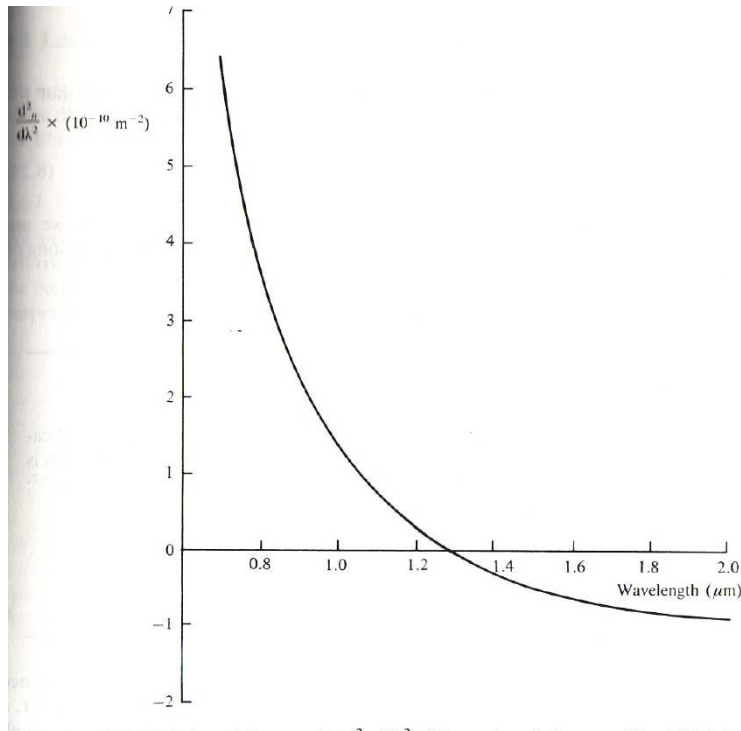


Figure 42: 2nd derivative term in silica

Waveguide dispersion arises from the fact that the mode velocity depends on $\beta(\lambda)$. This comes from the solution to Maxwell's equations in a cylindrical waveguide.

6.8 Losses in fibre optics

- bending losses
- intrinsic fibre losses

- impurities
- joins

Bending alters the TIR conditions at the fibre-cladding interface and at some critical radius of curvature the fibre will leak badly for a given mode. Another way of viewing this is to consider the wavefronts for a particular mode. At a bend wavefronts at large radii must travel faster than the speed of light to maintain phase. As this is not possible these wavefronts are radiated away.

The absorption constant associated with a bend is given by

$\alpha_R = C \exp(-R/R_c)$ where R is the radius of the bend and R_c is a critical radius. In practice

$$R_c = a/(N.A.)^2$$

and heavy losses don't occur before the fibre snaps. Bending losses are illustrated in Fig. 43.

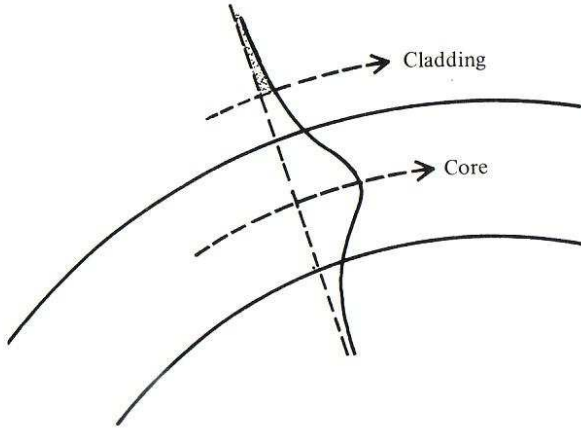


Figure 43: Bending losses occur when wavefronts are unable to maintain phase continuity.

Intrinsic scattering and absorption occurs because the material is inhomogeneous. If the refractive index varies over a length scale of $\approx \lambda/10$ then get Rayleigh scattering.

Impurities in the glass cause absorption. The pure silica contains traces of Fe^{3+} , Cu^{2+} and OH^- along with the doping material GeO_2 .

Joins are a major source of losses. Fresnel losses arise because of reflections at any air-glass interfaces. Losses obviously result if the fibres are not aligned to a common axis. Diffraction losses occur at any exit and entrance apertures.

$$R_F = (n_f - n_o)^2 / (n_f + n_o)^2$$

The reflection losses are reduced by excluding the air using a fluid with refractive index matched to the fibre material.

6.9 Communication using fibre optics

The potential advantages of fibre optics for use in communication systems are considerable:

- Very high frequency carrier so potentially very large bandwidth for information transfer. $\nu = 10^{14}$ Hz for $\lambda = 3\mu\text{m}$.
- Very compact. Both fibre links and the transmitters and receivers are small.
- Low cost.
- Low attenuation. They use very little power.
- Immune to electrical interference.
- Non-hazardous. There are no high voltages.

However they are not without their problems:

- Manufacture of low loss fibres is difficult.
- Modulation and subsequent demodulation of the light wave carrier is tricky and as yet the full bandwidth capability can't be realized. Lasers provide powerful light sources but are difficult to modulate at high switching rates. LED's are easier to modulate but produce less power.
- Joining fibres and repairing breaks is difficult.

The 2nd generation technology 1980's achieved up to ~ 1.7 G bits/sec. This is pushing the fibre, the source and the detector technology. We must work at $1.3\mu\text{m}$ to reduce attenuation and dispersion losses in silica fibres and hence the sources and detectors must work at this wavelength.

3rd generation working at $1.5\mu\text{m}$ up to ~ 2.5 G bits/sec by reducing dispersion in fibre and using narrower spectrum in source.

Higher rates achieved using improved multiplexing rather than better fibre, ~ 10 T bits/sec. Record 14 T bits/s.

6.10 Communication examples

A typical telephone conversation has a bandwidth of at least 0-4kHz i.e. $f_{max} = 4\text{kHz}$.

For digital encoding we require $8 \times 2 \times 4000 = 64$ kbits/sec using 1 byte per sample and two samples per period (the Nyquist rate).

Therefore a single link can transmit up to 25000 speech channels allowing for coding overheads, error trapping and so forth. Not bad for 1 fibre. However the limit set by the carrier frequency and dispersion in the fibre is $> 10^9$!

A DVD quality video is 5 Mbits/sec so can get may 100's of video streams in a single fibre.

7 Polarization

7.1 The linear polarizer

Such a device produces a \mathcal{P} -state from an unpolarized beam. Natural light \rightarrow linear light.

We can model natural light as 2 orthogonal \mathcal{P} -states which are *incoherent*, i.e. the phase difference between the states keeps changing. The *linear polarizer* removes or absorbs 1 of these states. The *axis* of the linear polarizer is defined by the plane of polarization of the resultant \mathcal{P} -state.

The effectiveness of a linear polarizer is indicated by the *extinction ratio*, the ratio of the min:max transmission (intensity) for a plane polarized beam.

7.2 The law of Malus

Suppose we have 2 linear polarizers in series as illustrated in Fig. 44. The first is called the polarizer and produces plane polarized light from an unpolarized beam. The second is called the analyser.

Let the angle between the axes of the polarizer and analyser be θ .

The \mathcal{P} -state produced by the polarizer can be resolved into \mathcal{P} -states \parallel and \perp to the axis of the analyser:

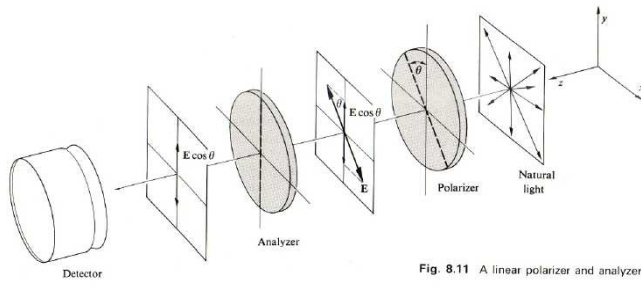


Fig. 8.11 A linear polarizer and analyzer—Malus's Law.

Figure 44: Using a polarizer and analyser

$$E_{\parallel} = E \cos \theta \text{ and } E_{\perp} = E \sin \theta.$$

The analyser will remove the E_{\perp} component leaving amplitude $E \cos \theta$. Hence the intensity is:

$$I(\theta) = I_o^2 \cos^2 \theta$$

This is the *law of Malus* named after Etienne Malus who published this relationship in 1809.

7.3 Dichroic crystals

Crystals which acted as linear polarizers were known to Newton. Materials which preferentially absorb one \mathcal{P} -state are said to be *dichroic* because the behaviour is dependent of colour (wavelength) and the crystals appear to have different colours depending on the illumination and direction of viewing.

Dichroism arises from a *complex refractive index* which depends on the direction of propagation - *anisotropy* of the refractive index.

Examples of naturally occurring dichroic crystals are tourmaline and herapathite. Within such crystals there is a specific direction (or directions) know as the *optic axis* (or optic axes).

Uniaxial crystals contain just 1 optic axis.

If the \underline{E} vector is \perp to this axis then the polarization state is stongly absorbed. So if the crystal is cut with a face \parallel to the optic axis and illuminated \perp to that face it acts as a linear polarizer.

The efficiency of the polarizer depends on the wavelength. e.g. if tourmaline is illuminated

by natural light normal to the principal optic axis it looks green (transmitted light) but if illuminated parallel to the same axis it looks pearly black. (2 colours - dichroic). The mineral hypersthene can look pink or green when illuminated by plane polarized white light.

This behaviour is caused by anisotropy in the electronic bonding structure of the crystal. Stiff bonds corresponding to a large restoring force per unit displacement have high resonance frequencies and weaker bonds have low resonance frequencies. Furthermore the bonds have different damping constants. This leads to different refractive indices for different directions in the crystal. Dichroic behaviour arises when the damping (absorption) is particularly strong for some directions.

7.4 Complex refractive index

The phase velocity is given by $v = d\omega/dk$ and the refractive index by $n = c/v$. Therefore:

$$k = \omega n/c$$

An harmonic travelling wave is given by:

$$A \exp i(\omega t - kz) = A \exp i(\omega t - \omega n z/c)$$

If the refractive index is complex then:

$$n = n_R + i n_I$$

If we substitute this into the functional form of the harmonic travelling wave we get:

$$A \exp i(\omega t - \omega n_R z/c) \exp(\omega n_I z/c)$$

The first exponential term propagates at $v = c/n_R$ and the second exponential term produces an exponential decay (absorption) or increase (amplification) depending on the sign of n_I . The absorption constant is $\alpha = 2\omega n_I/c \text{ m}^{-1}$. (Factor of 2 because energy flux is proportional to amplitude squared).

7.5 The wire grid polarizer

The simplest form of linear polarizer appeals directly to the electromagnetic nature of light. It consists of a grid of parallel conducting wires with a spacing d order of the wavelength.

The \underline{E} vector parallel to the wires is strongly attenuated because currents are induced. It is tempting to imagine that the \underline{E} vector slips between the wires. On the contrary it is the plane of polarization perpendicular to the wires that is transmitted.

If $d < \lambda/2$ then reflection is strong.

If $d \gg \lambda$ then transmission of both polarizations is high.

Such devices are most useful at large wavelengths (μ -waves) because of fabrication problems at optical wavelengths.

7.6 Dichroic sheet - Polaroid

Synthetic dichroic material, dichroic sheet or *polaroid* was invented by Herbert Land in 1928.

He first used synthetic herapathite (named after W. Herapath who discovered it).

Polaroid J-sheet is made from finely ground, needle like herapathite crystals aligned on a substrate. The crystals are ground small to reduce the scattering but J-sheet still looks milky.

Polaroid H-sheet invented by Land in 1938 is the molecular analog of the wire grid. Polyvinyl alcohol is stretched in 1 direction to form a sheet in which the chain molecules are aligned. It is then doped (soaked) with iodine ink to make the molecules conducting. The high transmission is perpendicular to the stretching direction. H-sheet does not suffer from scattering but is not very good at the blue end of the spectrum.

Modern developments e.g. K-sheet and HR-sheet improve the spectral range.

Linear Polarizer	Extinction ratio
calcite	10^{-7}
polaroid	10^{-3} to 10^{-5}
tourmaline	10^{-3}
wire grid	10^{-2}

7.7 Polarization by scattering - dipole scattering

From EM theory the radiation E-field from an oscillating dipole at a distance $r \gg \lambda$ is:

$$\underline{E} = \frac{k^2[P] \sin \theta}{4\pi\epsilon_o r} \hat{\theta}$$

where $[P]$ is the dipole moment at the retarded time $t' = t - r/c$.

$[P] = ql_o \exp i\omega(t - r/c)$ where q is the charge and l_o is the maximum separation. c.f. the previous expression for a current element in a half wavelength dipole. In that case we expressed the field in terms of a current which introduced a factor of $i\omega$.

The geometry is shown in Fig. 45.

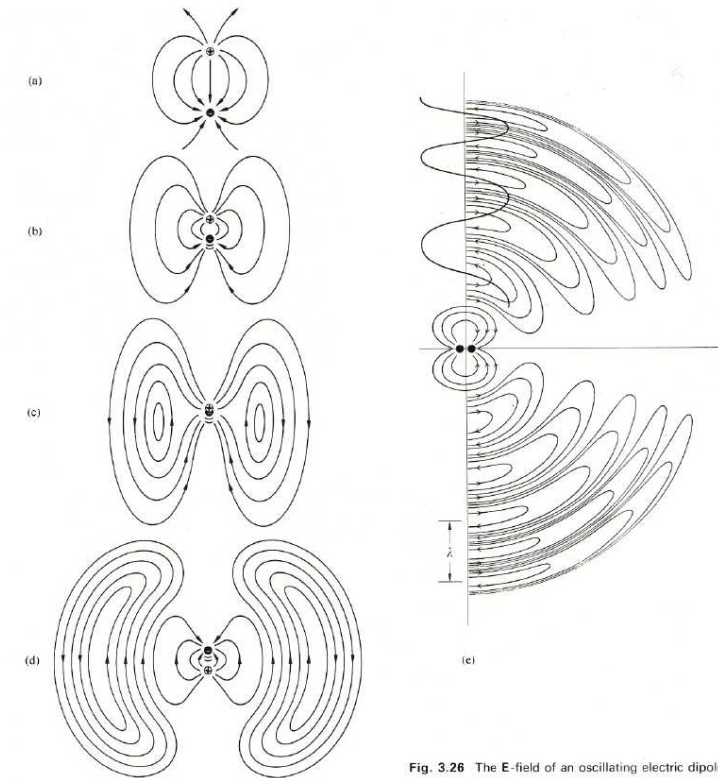


Fig. 3.26 The E-field of an oscillating electric dipole.

Figure 45: Radiation pattern from an oscillating dipole

Similarly the magnetic field strength of the radiation field is:

$$\underline{H} = -\frac{ck^2}{4\pi r} [P] \wedge \hat{r}$$

which is perpendicular to \underline{E} .

So the Poynting vector $\underline{N} = \underline{E} \wedge \underline{H}$ is proportional to k^4 .

Thus the intensity of scattering from a simple dipole is $\propto 1/\lambda^4$. This is called *Rayleigh Scattering*. It occurs when the dimensions of the scatterer are small compared with the wavelength of the EM radiation.

Rayleigh scattering gives us blue sky and red sunsets. Fine particles in the atmosphere scatter strongly at the blue end of the spectrum so viewing perpendicular to the solar radiation we see blue.

The radiation scattered through 90° is plane polarized because the \underline{E} vector is in the $\hat{\theta}$ direction wrt the dipole. The geometry of the scattering is shown in Fig. 46.

7.8 Polarization by reflection

Fresnel's equations derived from EM theory give us the amplitude reflection coefficients from an interface between 2 media.

$$R_{\perp} = r_{\perp}^2 = [E_{or}/E_{oi}]_{\perp}^2$$

$$R_{\parallel} = r_{\parallel}^2 = [E_{or}/E_{oi}]_{\parallel}^2$$

$$r_{\perp} = \frac{n_i \cos \theta_i - n_t \cos \theta_t}{n_i \cos \theta_i + n_t \cos \theta_t}$$

$$r_{\parallel} = \frac{n_t \cos \theta_i - n_i \cos \theta_t}{n_t \cos \theta_i + n_i \cos \theta_t}$$

If we substitute for the refractive indices using Snell's law:

$$r_{\perp} = -\frac{\sin(\theta_i - \theta_t)}{\sin(\theta_i + \theta_t)}$$

$$r_{\parallel} = \frac{\tan(\theta_i - \theta_t)}{\tan(\theta_i + \theta_t)}$$

When $\tan(\theta_i + \theta_t) \rightarrow \infty$, $r_{\parallel} \rightarrow 0$

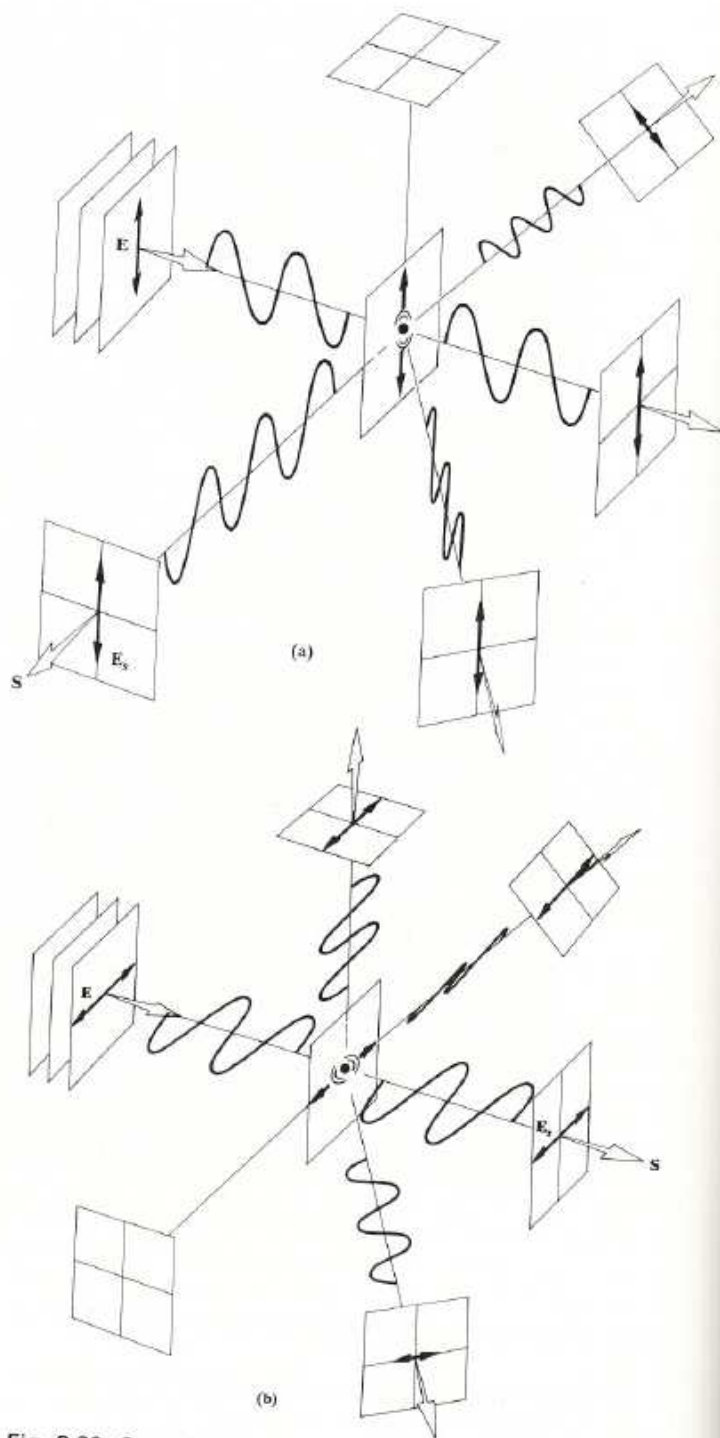


Fig. 8.36 Scattering of polarized light by a molecule.

Figure 46: Scattering of P-state by a molecule.

$\theta_t = 90 - \theta_i$ so $\sin \theta_t = \cos \theta_i$

but $n_i \sin \theta_i = n_t \sin \theta_t$ so:

$\tan \theta_B = n_t/n_i$ where θ_B is Brewster's angle.

If the \underline{E} vector is in the plane of reflection (parallel) then no reflection occurs at $\theta_i = \theta_B$.

8 Optical anisotropy

8.1 Birefringence - double refraction

If a material is optically anisotropic, the refractive index n varies with direction and *birefringence* or *double refraction* can occur.

The best known example of a birefringent material is the crystalline form of $CaCO_3$, calcite. The structure is shown in Fig. 47.

Within the crystal structure the carbonate groups lie in planes which are perpendicular to the optic axis.

The O atoms either appear in planes or distributed depending on the viewing direction wrt the crystal optic axis.

Calcite cleaves along 3 planes to form rhomboid crystals. However the optic axis is not perpendicular to any of the planes.

If a light rays impinges normal to any face 2 rays (beams) are generated in the crystal:

- The *ordinary ray* which passes straight through as expected (hence the name). It is plane polarized with the E vector perpendicular to the optic axis.
- The *extraordinary ray* which is refracted. It is plane polarized with the E vector in the plane containing the e-ray and the o-ray.

These rays are shown in Fig. 48.

The o-ray behaves as expected. Away from normal incidence refracted wavefronts are constructed using Huygens' principle in the usual way.

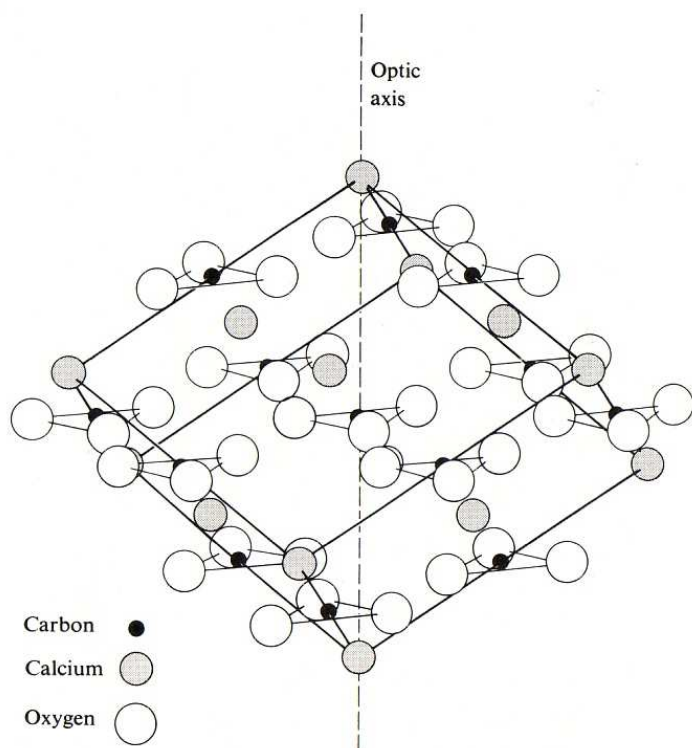


Figure 47: Structure of calcite

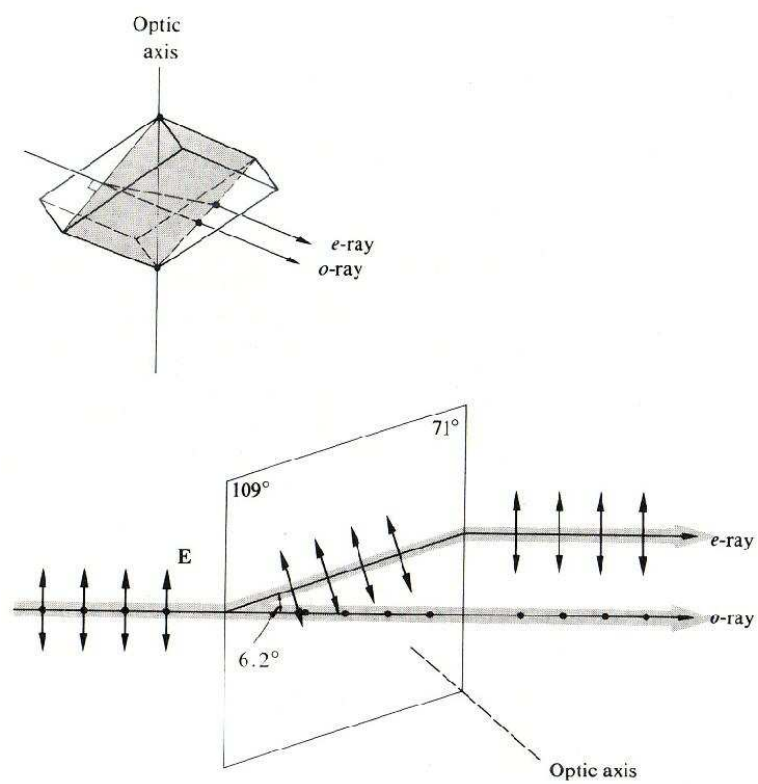


Figure 48: e-ray and o-ray in calcite

The e-ray behaviour is more complicated. The phase velocity is different parallel and perpendicular to the optic axis.

$$n_{\parallel} = 1.486 \text{ and } n_{\perp} = 1.658$$

The wavelets are ellipsoidal NOT spherical. The ray does not move perpendicular to the wavefronts!

The ray is defined by the direction of energy propagation. i.e. the Poynting vector, \underline{S} .

$$\underline{S} \perp \underline{E}$$

$$\underline{k} \perp \underline{D}$$

but \underline{E} is NOT \parallel to \underline{D} which means the polarization is NOT \parallel to \underline{E} . The wavelet construction for the o-ray and e-ray are shown in Fig. 49.

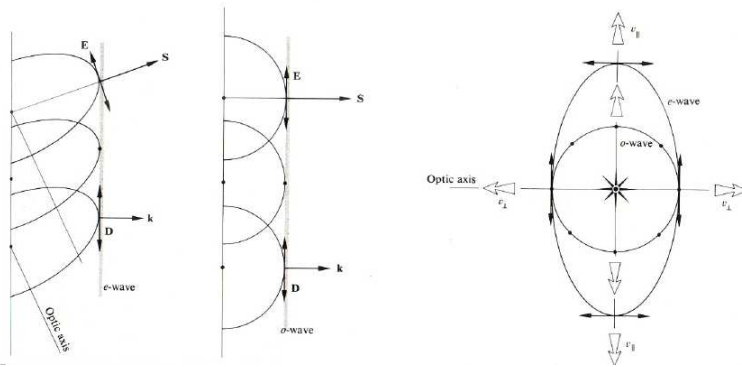


Figure 49: Wavelets of the e-ray and o-ray

Birefringent materials can be utilized to make very good linear polarizers. There are a number of cunning arrangements used to separate the o-ray and e-ray. The extinction ratio achieved from calcite can be $\approx 10^{-7}$.

8.2 Optical activity

In the above discussion of birefringence we might expect a ray propagating parallel to the optic axis, an o-ray, to exit unchanged. However in 1811 Arago discovered that quartz could rotate the plane of polarization of a \mathcal{P} -state beam. This behaviour is known as *optical activity*. It is illustrated in Fig. 50.

Such rotation takes place in some crystals, e.g. quartz, and some solutions, e.g. sugar

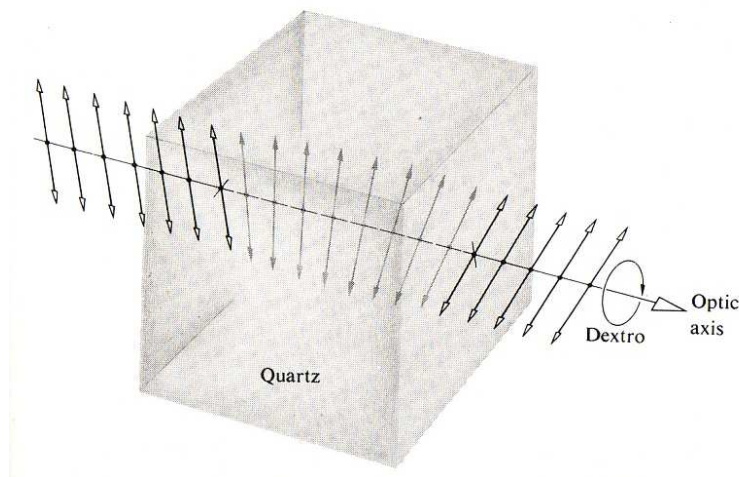


Figure 50: Optical activity in quartz

solutions. Some rotate to the left and some to the right.

- right - dextrorotatory
- left - levorotatory

This behaviour is dependant on wavelength. It is quantified as a *specific rotation*, rotation per unit length in the material.

It is due to the chiral nature, handedness, of either the crystal structure or the molecules themselves.

Molecules in solution can have a chiral characteristic independent of their orientation - c.f. a box of right handed screws. They are right handed screws whatever and exhibit mirror or reflection symmetry.

Optical activity arises because the refractive index is different for the circular \mathcal{R} and \mathcal{L} states.

$\mathcal{P} = \mathcal{R} + \mathcal{L}$ but the wavelength is slightly different for the component circular states so \mathcal{P} rotates.

In a liquid there is no optic axis and the rotation proceeds whatever the direction. However in an optically active crystal the polarization state that can propagate unchanged depends on the direction.

Schematically for any direction in an optically active crystal we can get 2 refractive indices

and 2 propagation states of polarization. We can plot the indices as a function of direction to generate *normal surfaces*. These surface are shown schematically in Fig. 51.

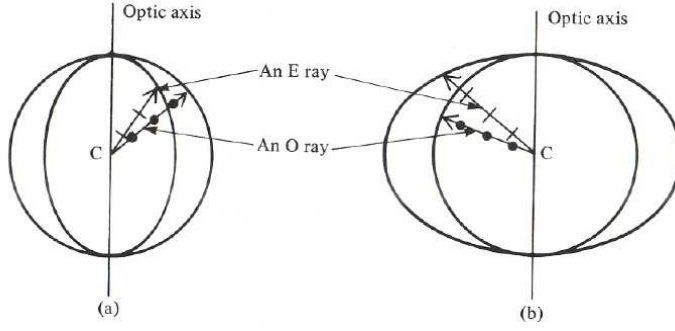


Figure 51: Wave propagation in an anisotropic medium - normal or index surfaces, (a) a positive and (b) a negative uniaxial crystal.

Along the optic axis the polarization states are \mathcal{R} and \mathcal{L} and in the case of quartz the normal surfaces don't meet. So in the direction of the optic axis these states propagate at different speeds hence we see optical activity. Note the separation of the normal surfaces on the diagram is exaggerated. It should be $\approx 0.6\%$ of the radius normal to the axis and $\approx 0.005\%$ parallel to the axis.

8.3 Retarders

Propagation perpendicular to the optic axis the polarization states are 2 orthogonal \mathcal{P} -states with the E vector parallel and perpendicular the axis. For a positive uniaxial material, e.g. quartz, the state in which E is parallel to the optic axis is *slow*. For a negative uniaxial material like calcite this is the *fast* direction. So for propagation perpendicular to the optic axis 1 \mathcal{P} -state is retarded wrt the other.

The path difference is given by:

$$\Delta = d(|n_o - n_e|) \text{ where } d \text{ is the distance through the crystal.}$$

Therefore the phase difference is:

$$\delta = \frac{2\pi}{\lambda} d(|n_o - n_e|)$$

Retarders are characterised by the phase difference they introduce between the \mathcal{P} -states with E vector perpendicular and parallel to the optic axis:

- $\delta = 2\pi$ - full wave plate - such a device is chromatic. Only 1 wavelength actually satisfies the required phase condition. That wavelength will propagate across the plate unaltered. Therefore when placed between crossed polaroids a full wave plate acts as a wavelength specific absorption filter.
- $\delta = \pi$ - half wave plate - if incoming plane polarized light is at an angle θ to the fast axis then it will rotate (flip) the plane through 2θ to $-\theta$. Similarly it will flip the major axis of elliptical light and invert the handedness of circular light.
- $\delta = \pi/2$ - quarter wave plate - if a \mathcal{P} -state is incoming at 45° to the optic axis then circular light will emerge and vice versa. At other angles the plate will transform a \mathcal{P} -state into an elliptical state.

Note that retardation plates have no effect if linear light is incident perpendicular or parallel to the optic axis since only 1 mode is excited. You only get a phase difference between 2 modes if there are 2 modes.

A half-wave plate is illustrated in Fig. 52.

9 Induced optical anisotropy

9.1 Faraday rotation - magnetically induced optical activity

In 1845 Michael Faraday discovered that the propagation of light through a medium could be influenced by the application of a strong magnetic field. At the time this was a strong indication that there was an intimate connection between light and electromagnetism.

If the applied \underline{B} field is parallel to the direction of propagation then the plane of polarization of linear light is rotated by an angle:

$$\beta = VBd$$

where V is the Verdet constant and d is the path length. V is a property of the medium and varies with temperature and the frequency of the light.

The theoretical treatment of the Faraday effect involves the quantum mechanical theory of the molecular electron energy levels in the presence of a magnetic field. A naive classical picture involves the magnetic force on the bound electrons. Such forces act radially on the orbiting electrons. The interaction alters the electric dipole moment of the electron and hence changes the dielectric constant, ϵ .

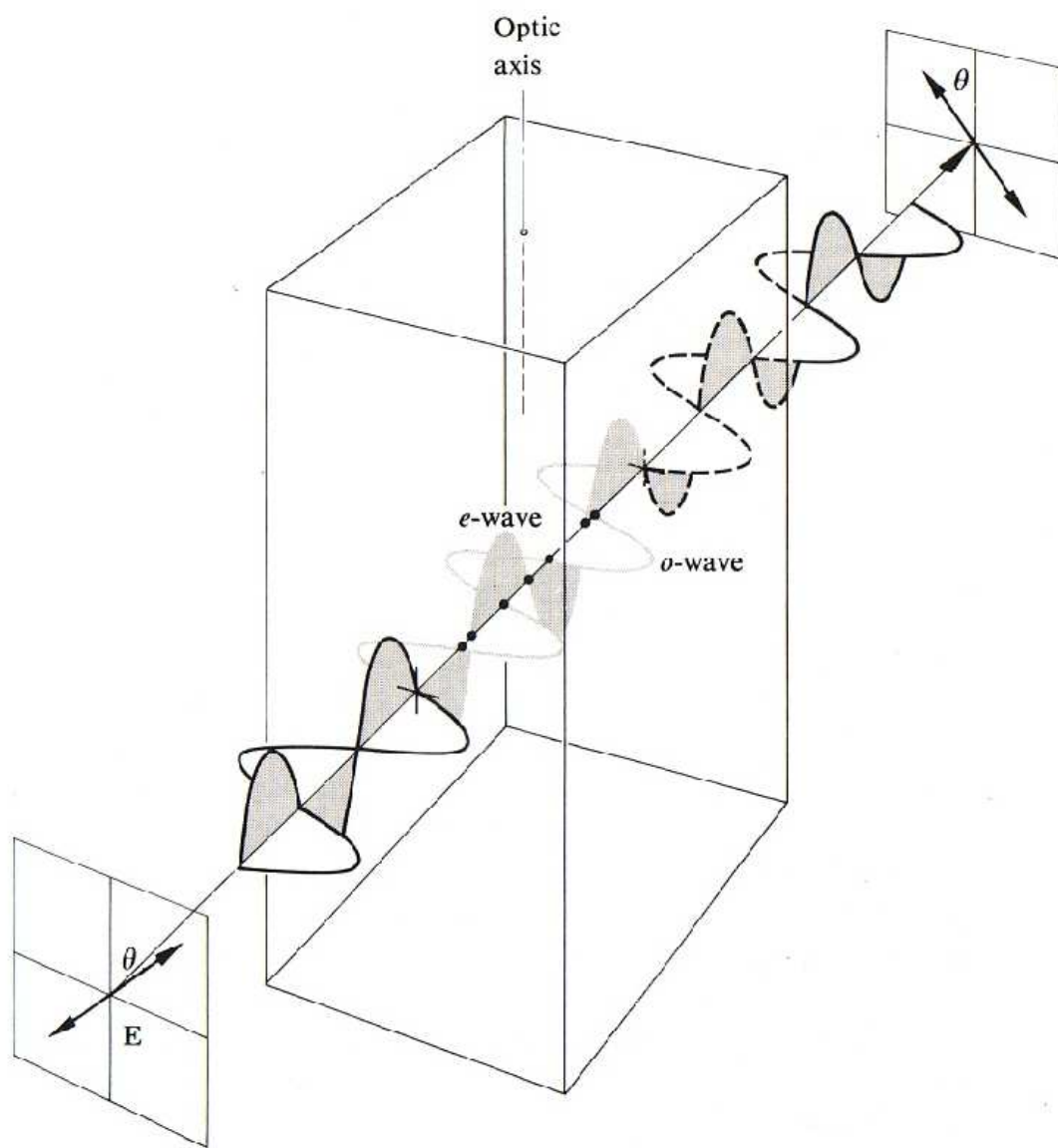


Figure 52: Half-wave plate

Under the influence of a beam of circular light the electrons are forced to circulate by the varying E field.

Thus in the presence of an applied B field and a circularly polarized light beam the electrons orbit at slightly different radii depending on the direction of the B field wrt the direction of propagation. We get two refractive indices n_R and n_L .

The circular components of a plane polarized beam travel at slightly different speeds and so the plane of polarization rotates - optical activity is induced by the magnetic field.

The plane of polarization is rotated in the same direction as the current required to generate the applied field if the Verdet constant is positive (diamagnetic).

Note the handedness of the rotation depends on the direction of the beam. This is different from *normal* optical activity.

Note also that in the case of magnetic materials the rotation angle β depends on the magnetization in the material not the applied field.

The Faraday effect can be utilized in a modulator. An infra read modulator can use YIG (magnetic yttrium iron garnet + gallium). This is illustrated in Fig. 53.

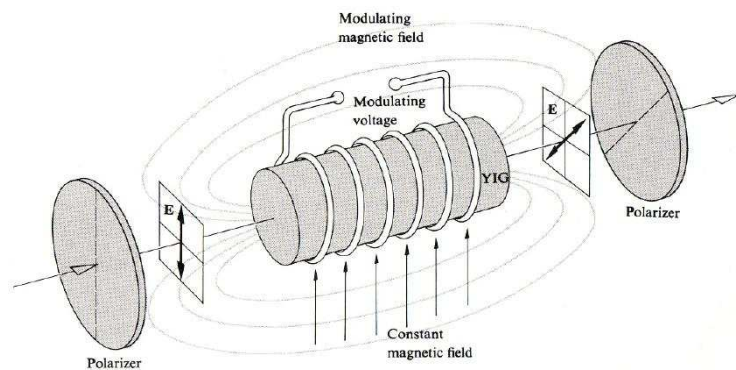


Figure 53: Faraday effect modulator

The specimen is saturated by a constant B field perpendicular to the axis and the parallel component is modulated using an axial coil. The rotation β depends on the modulated parallel field and the analyser samples according to the Law of Malus. Hence the laser beam is amplitude modulated.

The Faraday effect can also be used to produce an optical isolator - a device which transmits light in one direction but not the other. A Faraday rotating medium is placed between two polarizers set at 45° to each other. The magnetic field is set to give a rotation

of 45° so that a P-state beam is transmitted without loss. However if the beam is reversed the plane of polarization is rotated in the opposite direction (The B-field now points in the opposite direction wrt the propagation direction, see above) and therefore hits the second polarizer at 90° and is blocked.

There are also the Voigt (in vapour) and Cotton-Mouton (in liquid) magneto-optical effects in which the B field is applied perpendicular to the propagation direction and *birefringence* is induced in the material.

9.2 Liquid crystals

The passive digital liquid crystal display on your wrist watch is a fine example of useful optics.

The *liquid crystal state* is a *phase* occupied by many organic materials over a small range of temperature.

As the temperature increases the material passes from solid, through a liquid crystal phase (often with a milky appearance) to a clear liquid.

The material consists of *rod like* molecules that assume certain orientations with each other in the L.C. state.

A *director* is used to describe the preferred orientation in the L.C. state. This is a unit vector in the frame of reference of each molecule.

Three types of ordering occur, *nematic*, *cholesteric* and *smectic*.

Liquid crystals have the following properties:

- Under nematic ordering the directors are parallel to each other but the molecules are free to move as in a liquid.
- There is an ordering with respect to the liquid surface. Depending on the type of surface, rough, smooth, etc., the directors either lie parallel or perpendicular to the surface.
- The dielectric constant of the material depends on the direction of \underline{E} with respect to the directors ε_{\parallel} and ε_{\perp} . Thus since the molecules are free to move the application of an electric field changes the direction of the directors. If $\varepsilon_{\parallel} > \varepsilon_{\perp}$ then have a positive material with minimum energy when directors are \parallel to the field. A critical field strength E_c is required to align the directors.

- The material exhibits strong optical activity because of the orientation of the directors.

The ordering is shown schematically in Fig. 54.

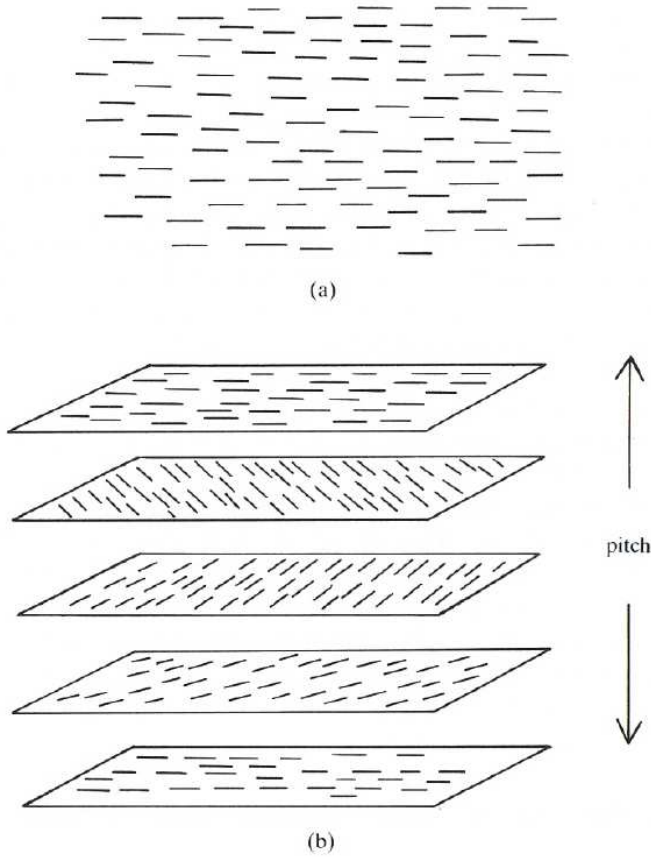


Figure 54: Order in liquid crystals, (a) nematic and (b) cholesteric.

We can use the above properties in what is called a *twisted nematic cell*. Liquid crystal is sandwiched between parallel plates.

The surface ordering property is used to twist the directors through 90° as they pass from one side of the cell to the other.

If a voltage is now applied between the plates such that $E > E_c$ directors in the bulk of the cell are forced parallel to the applied field.

When $V = 0$ a plane polarized beam passing across the cell will be rotated through 90° . When $V > E_c d$ a plane polarized beam is not effected as it passes through the cell. This is shown in Fig. 55.

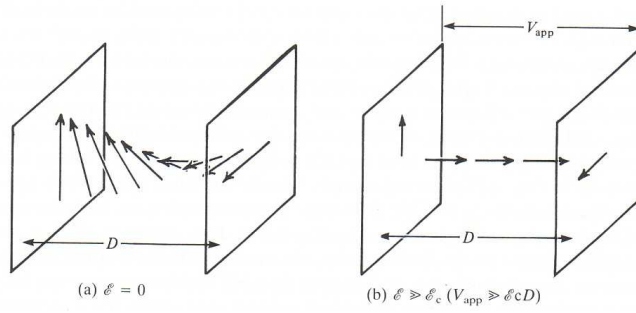


Figure 55: Operation of liquid crystals

We can place such a cell between two polarizers aligned to the ordering direction defined by the plate surfaces. A mirror is placed on one side of the cell.

Incident, unpolarized light is polarized on entry to the cell. If $V = 0$ the plane of polarization is rotated so that it is aligned with the other polarizer when it exits the cell. The mirror reflects the light and the beam travels back through the system. So if $V = 0$ we see a good reflection.

If $V > E_c d$ is applied the plane of polarization is not rotated by the liquid crystal and the beam cannot penetrate to the mirror so we see very little reflection.

So we can control the reflectivity using an applied voltage. In practice an A.C. waveform, $25 \rightarrow 1000 Hz$, is used and the cell reacts to the *r.m.s. voltage*. This gives the cell a much longer lifetime.

The action of an LCD cell is shown in Fig. 56.

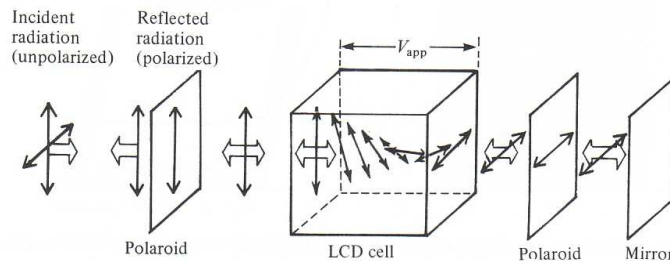


Figure 56: Action of Liquid Crystal Display

The now familiar LCD displays are:

- very low power
- rather slow

- brightness limited by reflectivity of polarized beam
- very versatile

The behaviour of the LC to an external field is an example of an *electro-optic effect*.

9.3 The Kerr and Pockels effects

The first electro-optic effect was discovered by John Kerr in 1875.

Birefringence can be induced by an electric field. Refractive indices n_{\parallel} and n_{\perp} are seen parallel and perpendicular to the field.

The difference in refractive index is given by:

$$\Delta n = \lambda_o K E^2$$

where K is the Kerr constant for the medium. Note the quadratic dependence on E . The effect is used in a *Kerr Cell* which can be used as an optical shutter.

If the applied voltage $V = 0$ then there is no transmission through the crossed polarizers. A V is applied birefringence is induced and the cell transmits.

Such shutters can be used to *Q switch* lasers.

Such switches can operate at a frequency of $\approx 10^{10} Hz$.

Kerr Cells act as a variable *wave plate*. Such a cell is illustrated in Fig. 57.

$$\Delta\phi = 2\pi K l V^2 / d^2$$

For example using the liquid nitrobenzene in a cell $d = 10mm$ and $l = 50mm$, if $V = 3 \times 10^4 V$ get a half wave plate.

Carl Pockels discovered a linear electro-optic effect in 1893. It is only seen in certain crystals that lack a centre of symmetry (and which are also piezoelectric).

A Pockels cell can be constructed in a similar way to the Kerr cell. They require only a tenth of the voltage of that needed for the Kerr cell and don't contain toxic liquid. The electric field is applied perpendicular (transverse) or parallel (longitudinal) to the direction of propagation depending on the crystal type. They have switching times of less

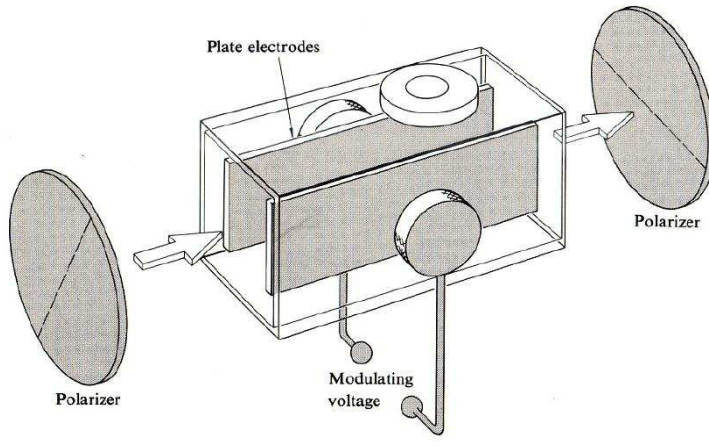


Figure 57: Kerr cell

than $10ns$ and can modulate at frequencies upto $25GHz$. A longitudinal cell is shown in Fig. 58. The phase retardance is given by:

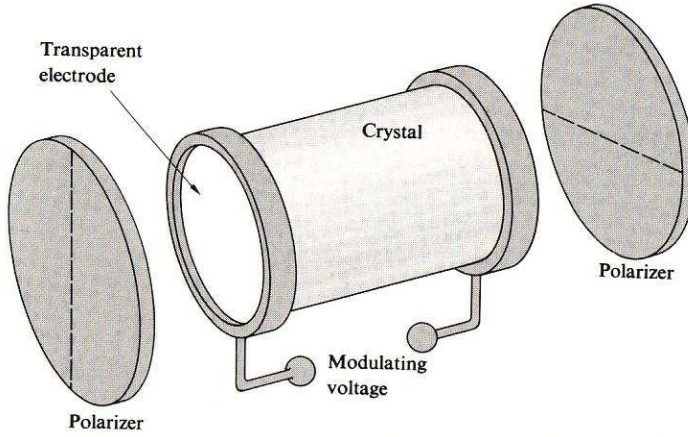


Figure 58: Pockels cell

$$\Delta\phi = 2\pi n_o^3 r_{63} V / \lambda_o$$

where r_{63} is the electro-optic constant in m/V , n_o is the refractive index, V is the applied potential and λ_o is the vacuum wavelength in metres.

An example of a suitable crystal is ammonium dihydrogen phosphate ($NH_4H_2PO_4$) ADP for which $r_{63} = 8.5 \times 10^{-12} m/V$, $n_o = 1.52$ at $\lambda_o = 546.1 nm$ and the voltage for a half wave plate is $V_{\lambda/2} = 9.2 kV$.

10 Nonlinear optics

Glass and similar dielectric materials have a dielectric constant or refractive index which is nonlinear. That is it depends on the electric field intensity. For example in fused quartz this is caused by the Kerr effect which has a response time of 10^{-15} seconds.

SiO_2 has a nonlinear refractive index of the form

$$n(\omega) = n_o(\omega) + i\chi(\omega) + n_2|E|^2$$

where $n_o = 1.5$, $n_2 = 3 \times 10^{-22} \text{ (V/m)}^{-2}$ and χ represents absorption.

10.1 Solitons

The transverse electric field of an EM-wave pulse travelling in an optical fibre has the form

$$E(x, r, t) = R(r) \text{Re}\{\phi(x, t) \exp(i(k_o x - \omega_o t))\}$$

where x is along the fibre, $R(r)$ is a radial eigenfunction and the phase velocity is given by $\omega_o/k_o = c/n_o(\omega_o)$. The function $\phi(x, t)$ is a complex envelope which is assumed to vary slowly compared with the carrier. Integrating over the radial coordinate the classical equation of motion of the envelope can be derived from Maxwell's equations and is given by

$$i\frac{\partial\phi}{\partial t} + i\omega_o'\frac{\partial\phi}{\partial x} + i\nu_o\phi + \frac{1}{2}\omega_o''\frac{\partial^2\phi}{\partial x^2} + \frac{\alpha\omega_on_2}{n_o}|\phi|^2\phi = 0$$

where $\omega_o' = \partial\omega_o/\partial k_o$, $\omega_o'' = \partial^2\omega_o/\partial k_o^2$, $\nu_o = \chi(\omega_o)\omega_o/n_o$ and α is approximately unity but depends on the radial profile of the electric field.

The second term gives the main group velocity of the envelope, the third term describes absorption, the fourth term describes further dispersion and the fifth term is the nonlinearity.

If the absorption term is zero and $\omega_o'' > 0$ (anomalous dispersion) and the nonlinearity is positive $n_2 > 0$ this wave equation has stationary pulse solutions of the form

$$\phi(x, t) = E_s \text{sech}\left(\frac{t - t_o - x/v_g}{\tau}\right) \exp(i(\kappa x - \Omega t))$$

where τ is the pulse width, t_o is the pulse centre and v_g is the pulse speed. The shape of the pulse does not change with time, that is there is no dispersion. The nonlinearity has effectively cancelled the effects of dispersion. The width of the pulse is inversely proportional to the maximum field intensity.

$$E_s^2 = \frac{n_o \omega_o''}{\alpha \omega_o n_2 v_g^2 \tau^2}$$

Note that the wavenumber and frequency of the carrier are modified (shifted) slightly by κ and Ω .

Using the values for the refractive index of SiO₂ if $\tau = 3$ ps and $f_o = \omega_o/(2\pi) = 4 \times 10^{14}$ Hz then in a fibre of cross-section $10\mu\text{m}^2$ the power in the pulse is 90 mW.

Such a pulse is called an optical soliton. It was predicted to be possible theoretically in 1973 and first demonstrated in 1980.

In 1988 soliton pulses were transmitted 4000 km error free using the Raman effect to overcome losses (provide optical gain).

In 1991 the record was extended to 14000 km using optical fibre amplifiers. Sections of fibre were doped with erbium and pumped to energise the optical pulses.

A so called solitary wave was first observed by J. Scott Russell on the Edinburgh- Glasgow canal in 1834. The equation which describes such a water wave was discovered by Korteweg and de Vries in 1895 and is referred to as the KdV equation.

$$\frac{\partial u}{\partial t} + v_0 \left(\frac{\partial u}{\partial x} + ru \frac{\partial u}{\partial x} + q \frac{\partial^3 u}{\partial x^3} \right) = 0 \quad (4)$$

This equation was originally analysed in the context of the irrotational two-dimensional flow of an incompressible inviscid fluid bounded above by a free surface and below by a horizontal plane. In other words waves in water of finite depth.

Soliton solutions to the KdV equation and optical solitons have the remarkable property that they interact strongly when they overlap but after the interaction they remain intact. They behave rather like particles.

10.2 Frequency doubling and mixing

In the linear, isotropic case the polarization in a dielectric is proportional to the electric field:

$$P = \epsilon_o \chi_e E$$

and the electric displacement is given by:

$$D = \epsilon_o E + P = \epsilon_o(1 + \chi_e)E = \epsilon_o \epsilon_r E$$

so the susceptibility is related to the permittivity:

$$\chi_e = \epsilon_r - 1$$

In a non-linear dielectric the polarization includes higher order terms of susceptibility:

$$P = \epsilon_o(\chi_1 E + \chi_2 E^2 \dots)$$

Therefore the E field from a light wave $E_o \cos \omega t$ induces a polarization of the form:

$$P = \epsilon_o(\chi_1 E_o \cos \omega t + \chi_2 (E_o \cos \omega t)^2 \dots)$$

or

$$P = \epsilon_o(\chi_1 E_o \cos \omega t + \frac{1}{2} \chi_2 E_o^2 (\cos 2\omega t + 1) \dots)$$

This polarization is oscillating at harmonic frequencies 2ω , 3ω etc. as well as the fundamental ω . The dielectric radiates at these higher frequencies. The second harmonic is readily produced in non-linear dielectrics - frequency doubling. Unfortunately dielectrics are also dispersive so that the different frequencies travel at different velocities and interfere. This limits the thickness of dielectric that can be used and hence the efficiency. However birefringent materials produce two waves in different directions and the direction of illumination can be chosen to reduce the interference leading to much higher efficiencies - e.g. potassium dihydrogen phosphate KDP can give a 30% yield in frequency doubling.

If two laser beams of different frequency ω_1 and ω_2 propagate in a non-linear dielectric then the non-linearity couples the two waves producing the sum and difference frequencies $\omega_1 - \omega_2$ and $\omega_1 + \omega_2$. This is called mixing.

In frequency doubling and mixing photons add (join) or subtract to form new photons. These processes need 2 photons and a molecule all close together so they only occur with high probability when the photon flux is very large (or equivalently when the E field is

very large).